
Efficient implementation of kernel filtering

Richard Beare¹ and Gaëtan Lehmann²

July 4, 2007

¹Department of Medicine, Monash University, Australia.

²INRA, UMR 1198; ENVA; CNRS, FRE 2857, Biologie du Développement et Reproduction, Jouy en Josas, F-78350, France

Abstract

Kernel based filtering is one of the fundamental tools of image analysis and processing. A number of approaches have been developed over the years that allow efficient implementation of such filters even when the kernel size is large. This article reviews some of these methods and introduces their ITK implementations.

Contents

1	Introduction	2
2	Separability and recursive implementations	2
3	Mathematical morphology operations	2
3.1	Arbitrary structuring elements	3
3.2	Decomposition of structuring elements	3
3.3	Line structuring elements	4
4	Rank filters	4
5	Mean and standard deviation filters	6
6	ITK implementation	8
6.1	Morphology filters – consolidatedMorphology	8
6.2	Rank and mean filters – fastRankMean	9
6.3	Rectangular convolution – boxConvolution	9
6.4	Extended languages support	10
7	Performance	10
7.1	Morpholgy	10
7.2	Rank and Mean filters	10
7.3	Box Convolution	10
7.4	Timing notes	10

8 Implementation Notes	13
8.1 Moving histograms	13
8.2 16 bit data types	13
8.3 Line Operations	13
8.4 Refactoring	13
9 Comments and Conclusions	14
10 Acknowledgments	14

1 Introduction

A kernel based filtering process replaces the pixel at the kernel origin with the result of a function of all pixels defined by the kernel. Many useful filters, including edge detection and gradient filters, smoothing filters and rank and morphology filters fall into this category. Direct implementations of such filters typically involve visiting all pixels defined by the kernel in order to evaluate the filter function. Such an approach is usually easy to implement – in ITK it is made simple by the neighborhood iterators – but leads to an algorithm complexity proportional to the number of pixels in the kernel (or $O(n^d)$, where n is the kernel size and d is the dimensionality). Such complexity tends to restrict application of such filters to small kernels.

A number of classical methods exist for reducing this complexity to more manageable, in some cases kernel size independent, levels. ITK already exploits such techniques for Gaussian convolution operations. This paper describes the classical techniques for optimized mathematical morphology filters, rank filters and certain convolution filters. These filters make the use of large kernels, which can be very useful in many applications, practical on conventional computing hardware.

2 Separability and recursive implementations

The two approaches most typically used to reduce complexity of kernel based filters are separability and recursive computation, both of which are used in the ITK implementation of Gaussian convolution filters. A separable filter implements a multidimensional kernel by cascading several one dimensional kernels, therefore reducing complexity from $O(n^d)$ to $O(nd)$. The second approach exploits redundancy that might be present in the computations of kernel functions at neighboring locations, leading, in some cases, to a complexity independent of n .

3 Mathematical morphology operations

Two optimized forms of the mathematical morphology operations of erosion, dilation, opening and closing are presented here. The kernel is usually referred to as the structuring element in mathematical morphology. The methods described here are applied to “flat” structuring elements, that is structuring elements without weights. The first method can be applied to arbitrary structuring elements while the second can be applied to line structuring elements.

3.1 Arbitrary structuring elements

The method described in [11] relies on the simple concept of an up-datable histogram, and is often described as a “moving histogram” approach. A histogram is computed for a kernel located at the first voxel. The histogram at the neighboring voxel can then be computed by including newly included voxels and removing newly excluded voxels. The list of included and excluded voxels corresponding to movement in any direction can be computed when the structuring element is created, and the direction with the smallest number of changes should be selected as the direction for sweeping the kernel across the image. The erosion or dilation at each location is computed by selecting the minimum or maximum from the histogram. This approach is very efficient when 8 or 16 bit pixels are used because the histogram can be represented as an array and the histogram updated by incrementing or decrementing the appropriate bins. Using place holders to track the current maximum or minimum increases performance. More sophisticated histogram representations are necessary for larger pixel types. Our implementation uses c++ maps, which is an extension to the original paper.

This methodology reduces the complexity from $O(n^d)$ to $O(n^{d-1})$, while keeping the structuring element identical to the direct implementation.

3.2 Decomposition of structuring elements

Morphological erosions and dilations are separable – successive dilation by orthogonal lines is equivalent to dilation by a rectangle with sides equal to the line lengths. This means that any hyper-rectangular structuring element can be constructed using several orthogonal lines, typically parallel to the axes.

Approximations of more complex shapes, notably circles and ellipses can be constructed using a number of lines at evenly spaced angles [2]. It is difficult to create a structuring element with a precisely defined radius using this method because line structuring elements from which the circle structuring element is composed must have odd length and there are practical limits due to the realities of underlying digital grid representation of images. In addition it is possible that the structuring elements may not be truly translation invariant due to the representation of line (e.g. Bresenham) used in the decomposition. However, precisely defined radii are rarely critical when a large structuring element is called for. An example of a structuring element created using line structuring elements is shown in Figure 1. Composition of regular shapes, such as hexagons and octagons is more accurate.



Figure 1: Approximate circular structuring element, radius 25, constructed using 8 lines.

It is also possible, in theory, to construct 3D structuring elements in similar ways. The construction of a hyper-rectangle is trivial, however construction of spheres is more problematic. The code discussed later provides preliminary implementations based on some platonic solids and various spherical approximations, but further testing and development is needed.

3.3 Line structuring elements

The decompositions discussed above are important because an efficient, recursive, implementation of erosion and dilations along lines exists. This method was introduced in [6, 12] and can compute an erosion or dilation in 3 operations per pixel, independent of structuring element length. [5] recently reduced the cost to 1.5 pixels per pixel, but the procedure is more complicated and there are reports of no speedup in practice.

The original algorithms utilize forward and backward running maxima (for dilation) for the length of the structuring element from a pixel of interest. The dilation can then be computed for a region the size of the structuring element around the point of interest by comparing values on the running extrema that are separated by the structuring element length. This is illustrated in Figure 2

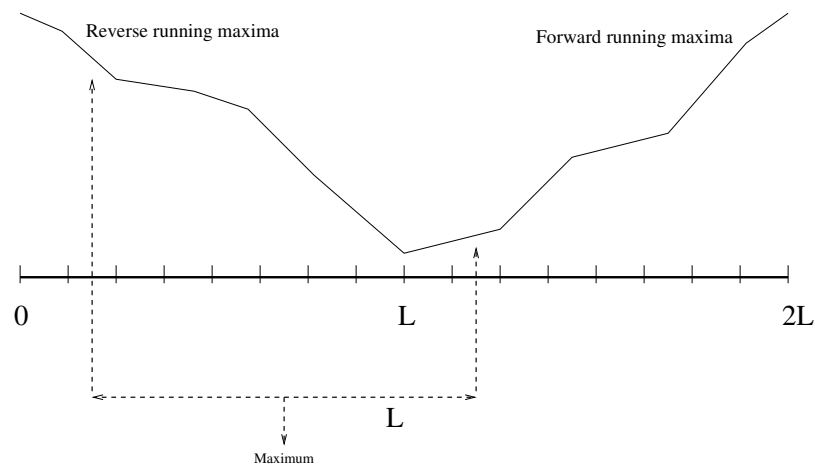


Figure 2: The van Herk, Gil, Werman method.

A method known as *anchor morphology* has been published recently [10] that offers improved performance and the ability to perform a line opening directly (rather than using an erosion/dilation cascade). This method has been implemented in the filters discussed later in the article, but performance issues are not yet clear. The method employs histograms and therefore needs more complex data structures when applied to higher precision data, potentially reducing any speed advantage.

4 Rank filters

Efficient implementations of median and rank filters can be carried out using exactly the same approach as discussed for morphological operations with arbitrary structuring elements. The method was originally proposed in [7]. The implementation discussed later supports arbitrary kernel shapes and pixel types as well as any choice of rank.

Rank filters are not separable. However the performance benefits offered by separability make it worth pretending they are. If median filtering is being used to provide robust noise filtering or background estimation then a separable approximation is worth testing. This concept was originally proposed in [9]. In fact it is also possible to apply the decomposition discussed in Section 3.2 to median filters to achieve a closer approximation to circular kernels.

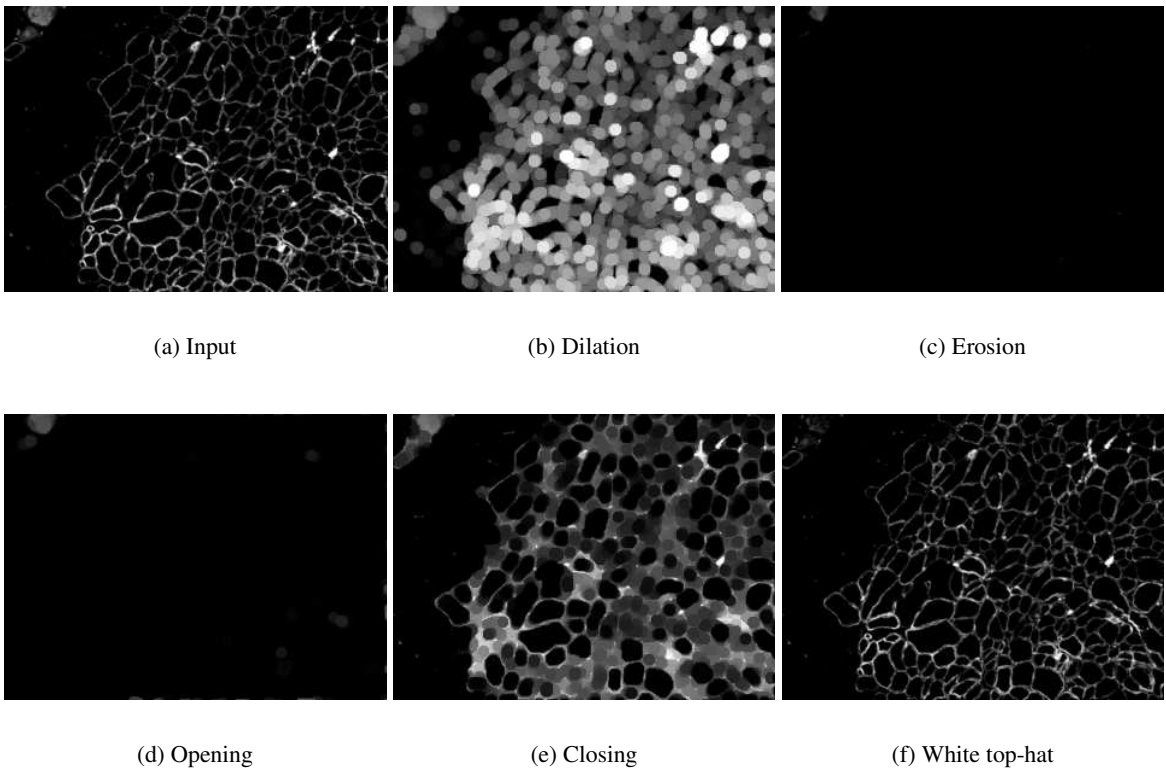


Figure 3: Effect of a dilation (b), an erosion (c), an opening (d), a closing (e) and a white top hat (f) with a ball structuring element.

5 Mean and standard deviation filters

A simplified version of the moving histogram approach can also be used to efficiently compute the mean or standard deviation of an arbitrarily shaped kernel. The histogram used for morphology and rank filters is a data structure that, once established for one pixel, can be easily updated to represent the kernel for a neighboring pixel. The data structure required to perform the equivalent function for mean and variance operations is much simpler – all that is necessary is the sum of pixel values under the kernel (or sum of squared values for variance calculations), and the kernel size. The sum can be updated by adding the new values and subtracting the old and the output computed by dividing by the kernel size.

A more efficient strategy was proposed in [3] for rectangular kernels. This approach first computes an accumulator image in which each i, j is replaced by the sum of voxels “left” and “above” it. This accumulator image may be computed recursively using local neighborhood values. The mean of rectangles of any size may then be computed using accumulated values at the rectangle corners. Figures 4 and 5 illustrate the 2D case and the update formulas are provided in Equations 1, 2, and 3.

$$\begin{aligned} b_{i,j} &= \sum_{x \leq i, y \leq j} a_{x,y} \\ &= b_{i,j-1} + b_{i-1,j} + a_{i,j} - b_{i-1,j-1} \end{aligned} \quad (1)$$

where $b_{i,j}$ is the accumulator value at location i, j and $a_{i,j}$ is the input image intensity at i, j .

$$S_{i,j} = b_{i+w/2, j+h/2} + b_{i-w/2, j-h/2} - b_{i-w/2, j+h/2} + b_{i+w/2, j-h/2} \quad (2)$$

where $S_{i,j}$ is the sum of the pixel values in the neighborhood centered at i, j .

$$m_{i,j} = \frac{1}{w \cdot h} S_{i,j} \quad (3)$$

where $m_{i,j}$ is the output of the mean filter at location i, j .

Using the same strategy, the standard deviation can be efficiently computed. It requires an accumulator image of the squared pixels values, which can be efficiently computed at the same time as the original accumulator image. The update formulas are provided in Equations 4, 5 and 6.

$$\begin{aligned} b2_{i,j} &= \sum_{x \leq i, y \leq j} a_{x,y}^2 \\ &= b2_{i,j-1} + b2_{i-1,j} + a_{i,j}^2 - b2_{i-1,j-1} \end{aligned} \quad (4)$$

where $b2_{i,j}$ is the accumulator value at location i, j for the square image, and $a_{i,j}$ is the input image intensity at i, j .

$$S2_{i,j} = b2_{i+w/2, j+h/2} + b2_{i-w/2, j-h/2} - b2_{i-w/2, j+h/2} + b2_{i+w/2, j-h/2} \quad (5)$$

where $S2_{i,j}$ is the sum of the squared pixel values in the neighborhood centered at i, j .

$$\sigma_{i,j} = \sqrt{\frac{S2_{i,j} - \frac{S_{i,j}^2}{w \cdot h}}{w \cdot h - 1}} \quad (6)$$

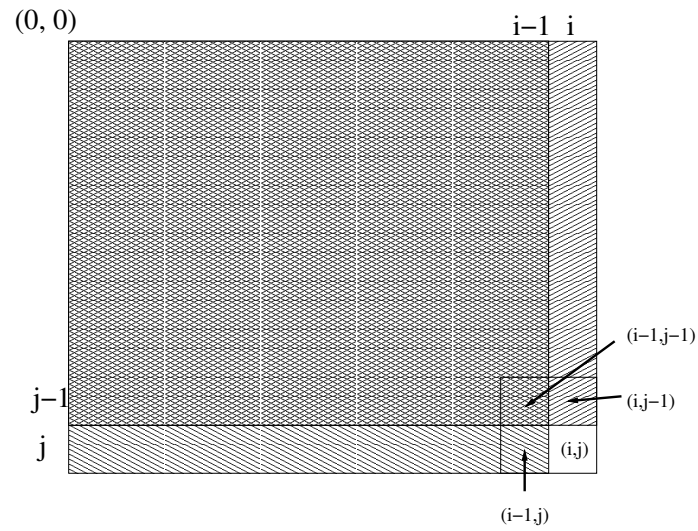


Figure 4: Recursive computation of the accumulator image - value at (i, j) computed using Equation 1. The double hashed region is subtracted because it is included in both $b_{i,j-1}$ and $b_{i-1,j}$.

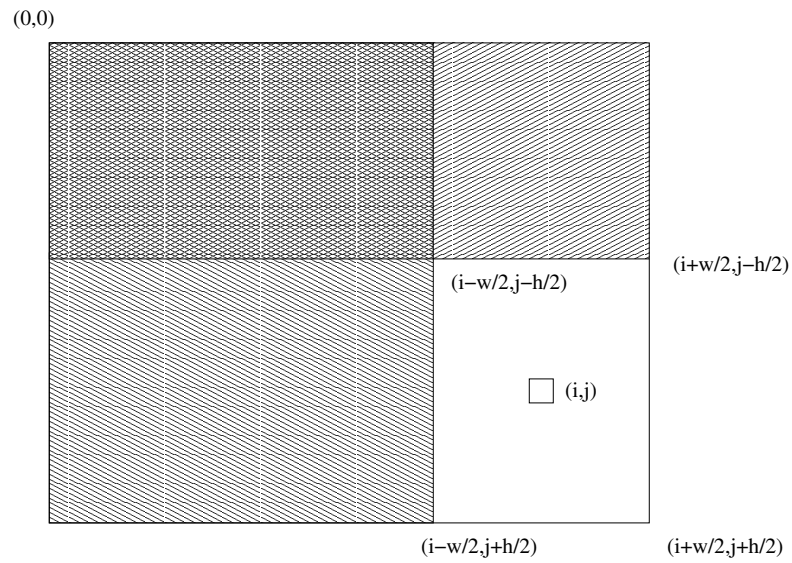


Figure 5: Computation of mean using the accumulated image - value at (i, j) computed using Equation 3.

where $\sigma_{i,j}$ is the output of the standard deviation filter at location i, j .

This approach to convolution has been used recently in face detection applications [13], where rectangular filters of many different sizes and shapes were needed and could be computed from the same accumulation image.

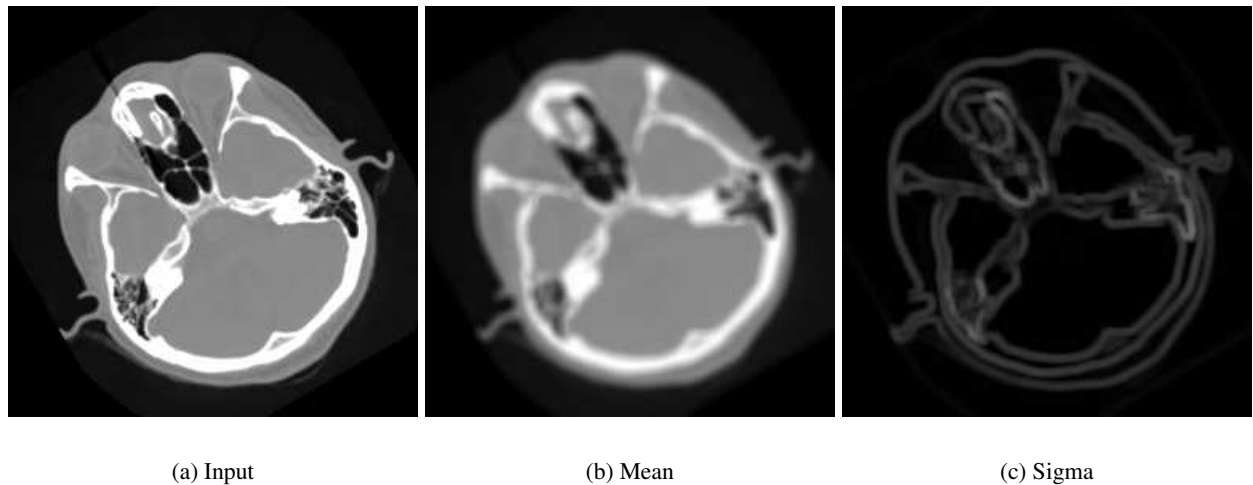


Figure 6: A mean transform (b) and a standard deviation transform (c) with a kernel of radius 3.

6 ITK implementation

The filters discussed in this article are contained in 3 packages – *consolidatedMorphology*¹, *fastRankMean* and *boxConvolution*. The most recent versions of these packages can be obtained from <http://voxel.jouy.inra.fr/darcsweb/2>. All of the packages include multithreaded filters and include many examples and tests. Unless indicated otherwise, all filters will behave basically the same way as other kernel filters, requiring either a radius or a neighborhood to be specified.

6.1 Morphology filters – consolidatedMorphology

The morphology filters utilize a new class – *FlatStructuringElement* to describe, arbitrary and decomposable structuring elements. It provides the following methods to create structuring elements with different characteristics:

- `Ball()` generate a ball structuring element (a circle in 2D). It takes the radius of the structuring element as parameter.
- `Box()` produces a box structuring element. It takes the radius of the structuring element as parameter.

¹An earlier version of the *consolidatedMorphology* package has been submitted to the InsightJournal. However many improvements and bug fixes have been included since then.

² The most recent versions can be obtained using darcs [1] with the command `darcs get http://voxel.jouy.inra.fr/darcs/contrib-itk/package`, where `package` must be replaced by *consolidatedMorphology*, *fastRankMean* or *boxConvolution*.

- `Poly()` produces an approximation to a circle or sphere using line structuring elements, taking the desired radius and number of lines as parameters. In the 3D case an approximation of a sphere will be attempted. Caution is advised because this is not well tested yet.
- `FromImage()` produces a structuring element from an image. The image is passed as parameter to the method. A optional parameter can also be passed: the pixel value to be considered as the foreground value in the image. This value defaults to `NumericTraits< PixelType >::max()`. This lets the user visualize the structuring element.

The algorithm used by a filter is set by the *SetAlgorithm* method, with options of *BASIC*, *HISTO*, *VHGW* and *ANCHOR*, for the traditional ITK implementation, the moving histogram algorithm, the van Herk, Gil, Werman algorithm and the anchor algorithm respectively. The VHGW and ANCHOR algorithms can only be used for Box and Poly structuring elements. VHGW is more thoroughly tested. The HISTO algorithm produces the identical results to BASIC, and is always faster. It is the default and should be used if you need precisely defined, non rectangular, structuring elements. If a Box structuring element is needed then VHGW or ANCHOR should be used, as they offer the best performance and are exact in that case. Poly structuring elements are approximations of circles that will offer improved performance with VHGW or ANCHOR algorithms, but the user will need to consider whether the approximation is suitable for the application in question.

The availability of line morphology operations means that new operations, such as “union of openings” can be implemented easily.

6.2 Rank and mean filters – fastRankMean

The *fastRankMean* package uses the sliding window method to implement rank and mean filters for arbitrary kernel shapes. It also uses line versions of these kernels to provide a “separable rank” filter – an fast approximation to a real rank filter as discussed in Section 4. There are also a number of filters that accept a mask input and return the rank or mean value of the intersection of kernel and mask. These are experimental and haven’t been thoroughly tested. The filters are *itkRankImageFilter*, *itkMovingWindowMeanImageFilter*, *itkFastApproxRankImageFilter*, *itkFastApproxMaskRankImageFilter* and *itkMaskedRankImageFilter*. *itkRankImageFilter* implements arbitrary shaped kernels, *itkFastApproxRankImageFilter* implements the separable approximation and *itkMovingWindowMeanImageFilter* implements an arbitrary shaped kernel mean.

6.3 Rectangular convolution – boxConvolution

The *boxConvolution* uses the accumulation method described in Section 5 to implement rectangular mean and variance computations. The filters implement different boundary conditions to *itkMeanImageFilter*, with the mean of the kernel inside the image being computed. The filters in this package are multithreaded and deal with arbitrary dimensions. The current filters do not support the mode of operation used in face recognition application in which an accumulation image is repeatedly “queried” for mean values of various sized kernels. However introducing such a capability is relatively easy.

6.4 Extended languages support

All the new filters provided are wrapped using WrapITK's external projects [4] and have been successfully tested with python.

7 Performance

All the execution times in this section are measured on a computer with four Intel®Xeon®CPU cores at 2.33GHz with 4MB cache, running CentOS 4.4 64 bits. Unless specified in the description, the tests are forced to run on a single core.

7.1 Morphology

Execution times for the dilation, the opening, and the gradient transform are shown in Tables 1, 3 and 2, and in Figure 7. The predicted linear complexity for the number of neighbors is observed for the basic algorithm, as well as the constant complexity of the van Herk / Gil Werman and the anchor algorithm. The linear complexity for the number of pixels added and removed per translation is observed for the moving histogram algorithm, as expected.

A good threading support is observed for all the implementations, as shown in Table 4 and Figure 7.

7.2 Rank and Mean filters

Relative times for sliding window median and mean filters and separable median filters are shown in Tables 6 and 7 and in Figure 8. The predicted linear complexity is observed for the sliding window approaches (complexity of direct approach is $O(n^2)$ in 2D, reduced to $O(n)$ by using the sliding window. The separable median exhibits a runtime independent of kernel size, as expected.

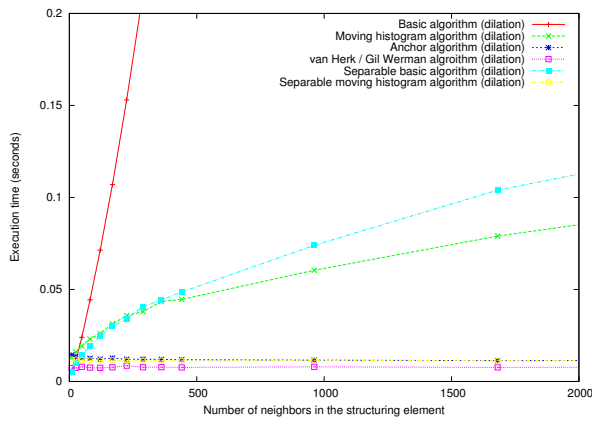
7.3 Box Convolution

The relative times for optimized and standard convolution are shown in Table 8 and Figure 9, and demonstrate significantly improved performance for kernel radii greater than 1. The times support the theoretical prediction that the complexity of the algorithm is independent of kernel size.

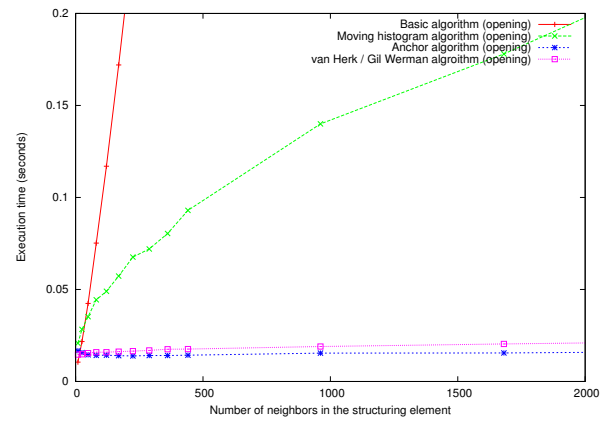
A good threading support is observed for all the implementations, as shown in Table 9 and Figure 9.

7.4 Timing notes

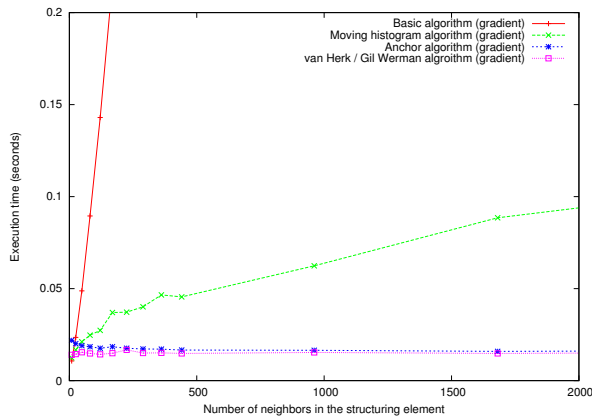
You may have noticed that the optimized filters of radius 1 seem to regularly perform slower than their larger counterparts. We can think of no reason for this. The algorithms that have kernel size independent complexity should not be slower for small kernels than large ones because the only difference occurs at borders and when the sliding window is being created, and both situations favour small kernels. We can only guess that there are caching issues involved.



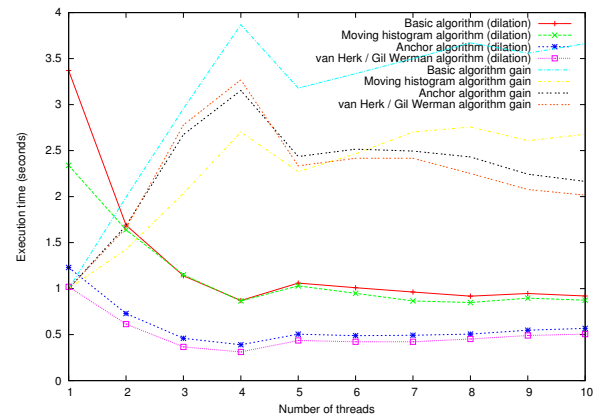
(a) Dilation



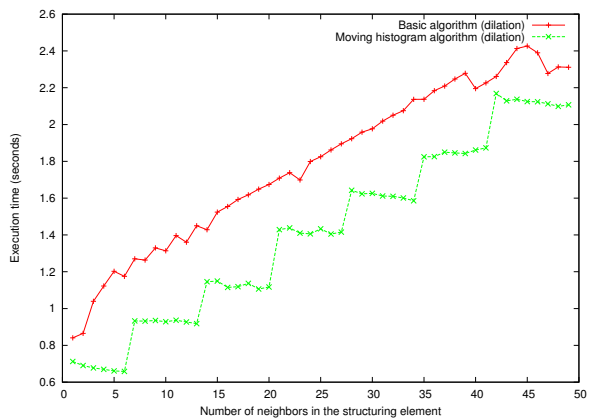
(b) Opening



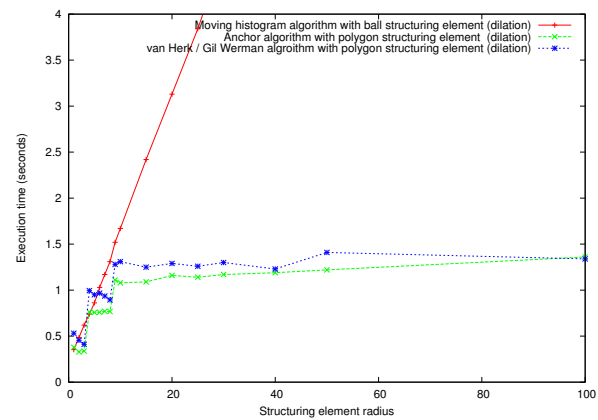
(c) Gradient



(d) Threads



(e) Number of neighbors



(f) Polygon

Figure 7: Execution times with a box structuring element of increasing size for different algorithms of dilation (a), opening (b) and gradient (c). Execution times with and increasing number fo threads (d). Execution times with an increasing number of neighbors in a box structuring of constant radius (e). Execution times with a polygon structuring element. The polygon approximations use the default number of lines (a maximum of 6 when radius is greater than 8 (f). Results are reported in Tables 1, 3, 2, 4 and 5.

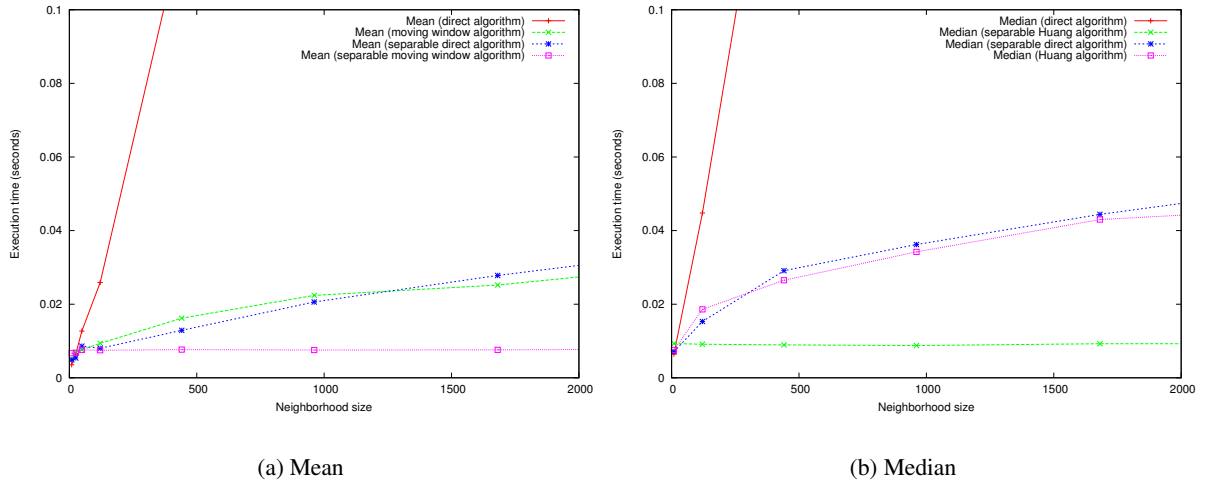


Figure 8: Execution times for several algorithms of mean filters (a) and median filters (b). Results are reported in Tables 6 and 7.

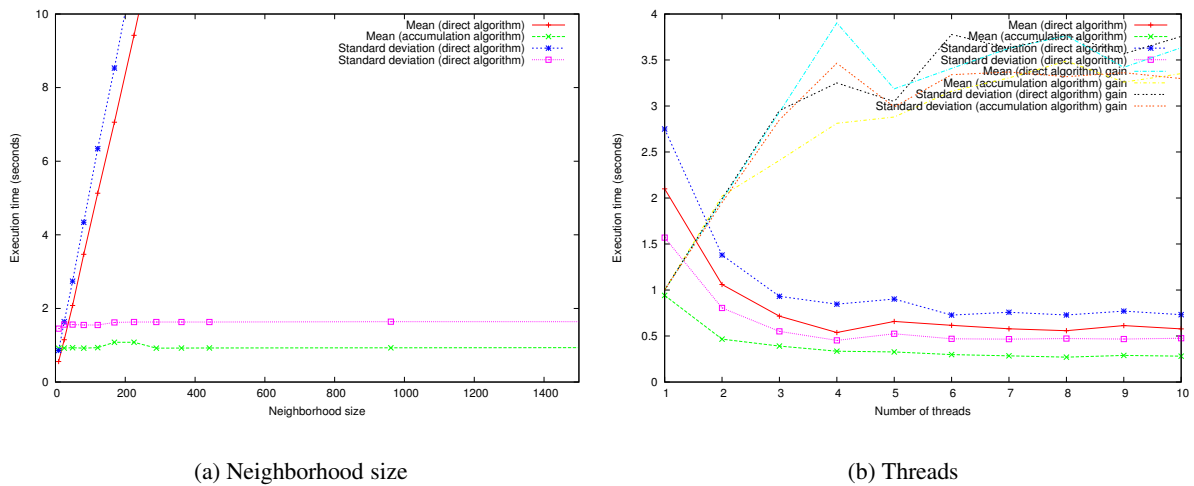


Figure 9: Execution times for and increasing kernel size (a), and an increasing number of threads (b). Results are reported in Tables 8 and 9

8 Implementation Notes

A lot of effort has been spent implementing and optimizing these filters while attempting to maintain good ITK style. This section summarizes some observations and experiences:

8.1 Moving histograms

The most obvious way of implementing moving histograms involves neighborhood iterators. However the resulting performance wasn't good – it appears that neighborhood iterator complexity is proportional to radius rather than the number of active neighbors. A method using lists of offsets combined with image Get/SetPixel methods approach was used instead.

The original paper recommended moving the window in a zig-zag pattern, i.e horizontally across a the first row, down a step to the second row and then back, but this involves accessing data in a reverse raster order which can potentially reduce cache performance. An alternative has been implemented that always moves the window in forward raster direction, at the cost of additional histogram copies, has been implemented and exhibits improved performance for large images. Differences for small images weren't detectable.

8.2 16 bit data types

Histograms for 16 bit data types can be implemented using arrays or maps. One would expect arrays to offer a simpler and therefore faster implementation, but our results have been mixed. Presumably the performance depends significantly on voxel statistics.

8.3 Line Operations

The van Herk/Gil and Werman and anchor methods operate on image transects, potentially at any angle. The transect data needs to be extracted from the image and the processed transect written back, with successive parallel transects being processed. Existing iterators don't do this particularly efficiently, so image Get/SetPixel operations are being used. This approach isn't ideal either and needs to be worked on. In general there is no need for boundary checks because the intersection between transect and image region is calculated, so a potentially random access method without boundary checks would be ideal.

Building dimension independent code also adds complexity to this filter which can be avoided in dimension specific implementations. The process of sweeping the transect across the image region is much more complex (and therefore slower) when written in a dimension independent fashion.

The standard ITK threading approach isn't ideal for this style of filtering either – a better option would be splitting the image based on transects instead of blocks. Obviously this sort of change isn't practical.

8.4 Refactoring

The three packages do share some components, and some refactoring is called for. This most widely used components are histograms and sliding window infrastructure, which need to be consolidated.

All the kernel based filters in ITK would also benefit to hinerit a common super class which manage the neighborhood size and/or the kernel, and which provide the infrastructure for the separable operations.

9 Comments and Conclusions

This article has provided background theory for and implementations of a number of important approaches to kernel based filtering. These methods significantly reduce complexity and execution time, by some orders of magnitude in many cases. These approaches are all well established in the literature but weren't available in ITK. Availability of filtering algorithms which are always fast, irrespective of the kernel size, can make much simpler approaches to many problems practical.

10 Acknowledgments

We thank Dr Pierre Adenot and MIMA2 confocal facilities (<http://mima2.jouy.inra.fr>) for providing the 3D test image. We are grateful to the INRA MIGALE bioinformatics platform (<http://migale.jouy.inra.fr>) for providing the computational resources used for the timing tests.

References

- [1] <http://www.darcs.net>. 2
- [2] R. Adams. Radial decomposition of discs and spheres. *CVGIP: Graphical models and image processing*, 55(5):325–332, September 1993. 3.2
- [3] F.C. Crow. Summed-area tables for texture mapping. In *SIGGRAPH '84: Proceedings of the 11th annual conference on Computer graphics and interactive techniques*, pages 207–212, New York, NY, USA, 1984. ACM Press. 5
- [4] Zachary Pincus Gaëtan Lehmann and Benoit Regrain. Wrapitk - enhanced languages support for the insight toolkit. *Insight Journal*, January - June 2006. 6.4
- [5] J. Gil and R. Kimmel. Efficient dilation, erosion, opening and closing algorithms. In *Mathematical Morphology and its Applications to Image and Signal Processing*, pages 301–310. Kluwer Acad. Pub, 2000. 3.3
- [6] J. Gil and M. Werman. Computing 2-d min, median, and max filters. *IEEE Transactions on Pattern Analysis and Machine Intelligence*, 15(5):504–507, May 1993. 3.3
- [7] T.S. Huang, G.Y. Yang, and G.Y. Tang. A fast two-dimensional median filtering algorithm. *IEEE Transactions on Acoustics, Speech and Signal Processing*, 27:13–18, 1979. 4
- [8] L. Ibanez and W. Schroeder. *The ITK Software Guide*. Kitware, Inc. ISBN 1-930934-10-6, <http://www.itk.org/ItkSoftwareGuide.pdf>, 2003.
- [9] P.M. Narendra. A separable median filter for image noise smoothing. *IEEE Transactions on Pattern Analysis and Machine Intelligence*, 3:20–29, 1981. 4
- [10] M. Van Droogenbroeck and M. Buckley. Morphological erosions and openings: fast algorithms based on anchors. *Journal of Mathematical Imaging and Vision, Special Issue on Mathematical Morphology after 40 Years*, 22(2-3):121–142, May 2005. Algorithms in ANSI C code are available in libmorpho. 3.3

- [11] M. Van Droogenbroeck and H. Talbot. Fast computation of morphological operations with arbitrary structuring elements. *Pattern Recognition Letters*, 17(14):1451–1460, 1996. 3.1
- [12] M. van Herk. A fast algorithm for local minimum and maximum filters on rectangular and octagonal kernels. *Pattern Recognition Letters*, 13(7):517–521, July 1992. 3.3
- [13] P. Viola and M. Jones. Robust real-time face detection. *International Journal of Computer Vision*, 57(2):137–154, 2004. 5

Appendix

Radius	Basic	Separable	Histogram	Separable histogram	Anchor	van Herk / Gil Werman
1	0.00477	0.00491	0.013	0.012	0.0144	0.00725
2	0.0114	0.0101	0.0161	0.0119	0.0135	0.00743
3	0.024	0.0146	0.0193	0.0116	0.0129	0.00794
4	0.0444	0.0192	0.0231	0.0114	0.0126	0.00755
5	0.0714	0.0247	0.0261	0.0114	0.0121	0.0074
6	0.107	0.0299	0.0313	0.0116	0.0127	0.00771
7	0.153	0.034	0.0358	0.0113	0.0121	0.00859
8	0.211	0.0407	0.038	0.0112	0.0121	0.00773
9	0.281	0.0442	0.0434	0.0114	0.012	0.00779
10	0.365	0.0486	0.0446	0.0111	0.0118	0.00763
15	1.03	0.074	0.0604	0.0115	0.0116	0.00794
20	2.23	0.104	0.079	0.0113	0.0113	0.00762
25	4.11	0.129	0.0968	0.0114	0.0116	0.0079
30	6.82	0.154	0.111	0.0114	0.0115	0.00781
40	15.4	0.214	0.153	0.0116	0.0116	0.00785
50	29.3	0.285	0.19	0.0119	0.0117	0.00804
100	226	0.767	0.355	0.0129	0.0117	0.00809

Table 1: Execution times in seconds for dilation by boxes using several algorithm implementations applied to the 256×256 cthead image.

Radius	Basic	Histogram	Anchor	van Herk / Gil Werman
1	0.0107	0.0124	0.0219	0.014
2	0.0235	0.0167	0.0201	0.0144
3	0.0488	0.0211	0.019	0.0154
4	0.0895	0.0247	0.0184	0.0148
5	0.143	0.0273	0.0176	0.0143
6	0.216	0.037	0.0184	0.0149
7	0.308	0.0372	0.0176	0.0167
8	0.423	0.0401	0.0172	0.015
9	0.563	0.0466	0.0171	0.0151
10	0.73	0.0455	0.0166	0.0148
15	2.07	0.0624	0.0165	0.0153
20	4.46	0.0885	0.0159	0.0148
25	8.22	0.104	0.0163	0.0153
30	13.6	0.118	0.0161	0.0151
40	30.9	0.153	0.0163	0.0153
50	58.6	0.196	0.0168	0.0156
100	452	0.339	0.0163	0.0157

Table 2: Execution times in seconds for morphological gradient transformation by boxes using several algorithm implementations applied to the 256×256 cthead image.

Radius	Basic	Histogram	Anchor	van Herk / Gil Werman
1	0.0105	0.0208	0.0167	0.0146
2	0.0217	0.0283	0.0157	0.0148
3	0.0424	0.0352	0.0145	0.0154
4	0.0752	0.0444	0.0142	0.0159
5	0.117	0.049	0.0143	0.0159
6	0.172	0.0573	0.014	0.0162
7	0.24	0.0676	0.0139	0.0165
8	0.324	0.072	0.0141	0.0169
9	0.425	0.0804	0.0141	0.0175
10	0.546	0.093	0.0143	0.0176
15	1.5	0.14	0.0154	0.019
20	3.19	0.178	0.0155	0.0204
25	5.9	0.235	0.0164	0.0219
30	9.9	0.274	0.0175	0.0236
40	23	0.383	0.0193	0.0272
50	45.3	0.522	0.0213	0.0298
100	421	1.6	0.0346	0.0493

Table 3: Execution times in seconds for morphological opening by boxes using several algorithm implementations applied to the 256×256 cthead image.

Threads	Basic	Histogram	Anchor	van Herk / Gil Werman
1	3.37	2.34	1.23	1.02
2	1.69	1.64	0.73	0.615
3	1.14	1.15	0.46	0.367
4	0.871	0.866	0.39	0.312
5	1.06	1.03	0.505	0.437
6	1.01	0.949	0.489	0.422
7	0.963	0.866	0.493	0.422
8	0.918	0.849	0.506	0.453
9	0.947	0.897	0.548	0.491
10	0.92	0.874	0.568	0.506

Table 4: Execution times in seconds for morphological opening by boxes using several algorithm implementations applied to the 3200×2400 image.

Radius	Histogram	van Herk / Gil Werma	Anchorn
1	0.354	0.379	0.532
2	0.486	0.329	0.455
3	0.62	0.338	0.411
4	0.74	0.763	0.995
5	0.862	0.757	0.95
6	1.03	0.759	0.968
7	1.17	0.77	0.936
8	1.31	0.768	0.894
9	1.52	1.11	1.28
10	1.67	1.08	1.31
15	2.42	1.09	1.25
20	3.13	1.16	1.29
25	3.84	1.14	1.26
30	4.64	1.17	1.3
40	5.95	1.19	1.23
50	7.6	1.22	1.41
100	19	1.36	1.34

Table 5: Execution times in seconds for morphological opening by boxes using several algorithm implementations applied to the 256×256 cthead image.

Radius	Direct	Moving window	Separable direct	Separable moving window
1	0.00355	0.00498	0.00487	0.00668
2	0.00642	0.00706	0.0054	0.00679
3	0.0127	0.00761	0.00861	0.00756
5	0.0259	0.00936	0.00803	0.00749
10	0.121	0.0162	0.0129	0.00765
15	0.35	0.0224	0.0206	0.00755
20	0.771	0.0252	0.0278	0.0076
40	5.59	0.059	0.0699	0.00871

Table 6: Execution times in seconds for mean filters using direct and sliding window implementations applied to the 256×256 cthead image.

Radius	Direct	Huang	Separable direct	Separable huang
1	0.00642	0.00758	0.0071	0.0093
5	0.0448	0.0186	0.0153	0.00913
10	0.177	0.0265	0.0291	0.00895
15	0.445	0.0342	0.0362	0.00876
20	0.93	0.043	0.0444	0.00925
40	6.21	0.061	0.0899	0.00936

Table 7: Execution times in seconds for median filters using direct and sliding window implementations applied to the 256×256 cthead image. The separable median is an approximation and therefore doesn't produce the same result as the direct or sliding algorithms.

Size	Direct Mean	Box Mean	Direct sigma	Box sigma
1	0.557	0.916	0.858	1.45
2	1.15	0.924	1.64	1.56
3	2.08	0.932	2.74	1.56
4	3.47	0.92	4.34	1.55
5	5.13	0.935	6.34	1.55
6	7.06	1.08	8.53	1.62
7	9.42	1.08	11.3	1.63
8	12.2	0.922	14.5	1.63
9	15.3	0.924	18	1.63
10	18.9	0.925	22.1	1.63
15	43.3	0.929	50.2	1.64
20	80.1	0.936	91.8	1.64
25	131	0.939	149	1.64

Table 8: Execution times in seconds for mean and standard deviation using direct and box convolution implementations applied to the 3200×2400 image.

Size	Direct Mean	Box Mean	Direct sigma	Box sigma
1	2.1	0.942	2.75	1.57
2	1.06	0.466	1.38	0.805
3	0.716	0.391	0.932	0.551
4	0.538	0.335	0.846	0.453
5	0.659	0.327	0.902	0.525
6	0.616	0.298	0.728	0.47
7	0.579	0.285	0.758	0.466
8	0.558	0.27	0.729	0.473
9	0.614	0.289	0.771	0.467
10	0.578	0.281	0.732	0.476

Table 9: Execution times in seconds for mean and standard deviation using direct and box convolution implementations applied to the 3200×2400 image.

Efficient implementation of kernel filtering

Richard Beare¹ and Gaëtan Lehmann²

August 15, 2007

¹Department of Medicine, Monash University, Australia.

²INRA, UMR 1198; ENVA; CNRS, FRE 2857, Biologie du Développement et Reproduction, Jouy en Josas, F-78350, France

Abstract

Kernel based filtering is one of the fundamental tools of image analysis and processing. A number of approaches have been developed over the years that allow efficient implementation of such filters even when the kernel size is large. This article reviews some of these methods and introduces their ITK implementations.

Contents

1	Introduction	2
2	Separability and recursive implementations	2
3	Mathematical morphology operations	2
3.1	Arbitrary structuring elements	3
3.2	Decomposition of structuring elements	3
3.3	Line structuring elements	4
4	Rank filters	4
5	Mean and standard deviation filters	6
6	ITK implementation	8
6.1	Common filters	8
6.2	Morphology filters – consolidatedMorphology	9
6.3	Rank and mean filters – fastRankMean	10
6.4	Rectangular convolution – boxConvolution	10
6.5	Extended languages support	10
7	Performance	10
7.1	Morpholgy	11
7.2	Rank and Mean filters	11
7.3	Box Convolution	11
7.4	Timing notes	11

8	Implementation Notes	11
8.1	Moving histograms	11
8.2	16 bit data types	14
8.3	Line Operations	14
8.4	Refactoring	15
9	Comments and Conclusions	15
10	Acknowledgments	15

1 Introduction

A kernel based filtering process replaces the pixel at the kernel origin with the result of a function of all pixels defined by the kernel. Many useful filters, including edge detection and gradient filters, smoothing filters and rank and morphology filters fall into this category. Direct implementations of such filters typically involve visiting all pixels defined by the kernel in order to evaluate the filter function. Such an approach is usually easy to implement – in ITK it is made simple by the neighborhood iterators – but leads to an algorithm complexity proportional to the number of pixels in the kernel (or $O(n^d)$, where n is the kernel size and d is the dimensionality). Such complexity tends to restrict application of such filters to small kernels.

A number of classical methods exist for reducing this complexity to more manageable, in some cases kernel size independent, levels. ITK already exploits such techniques for Gaussian convolution operations. This paper describes the classical techniques for optimized mathematical morphology filters, rank filters and certain convolution filters. These filters make the use of large kernels, which can be very useful in many applications, practical on conventional computing hardware.

2 Separability and recursive implementations

The two approaches most typically used to reduce complexity of kernel based filters are separability and recursive computation, both of which are used in the ITK implementation of Gaussian convolution filters. A separable filter implements a multidimensional kernel by cascading several one dimensional kernels, therefore reducing complexity from $O(n^d)$ to $O(nd)$. The second approach exploits redundancy that might be present in the computations of kernel functions at neighboring locations, leading, in some cases, to a complexity independent of n .

3 Mathematical morphology operations

Two optimized forms of the mathematical morphology operations of erosion, dilation, opening and closing are presented here. The kernel is usually referred to as the structuring element in mathematical morphology. The methods described here are applied to “flat” structuring elements, that is structuring elements without weights. The first method can be applied to arbitrary structuring elements while the second can be applied to line structuring elements.

3.1 Arbitrary structuring elements

The method described in [11] relies on the simple concept of an up-datable histogram, and is often described as a “moving histogram” approach. A histogram is computed for a kernel located at the first voxel. The histogram at the neighboring voxel can then be computed by including newly included voxels and removing newly excluded voxels. The list of included and excluded voxels corresponding to movement in any direction can be computed when the structuring element is created, and the direction with the smallest number of changes should be selected as the direction for sweeping the kernel across the image. The erosion or dilation at each location is computed by selecting the minimum or maximum from the histogram. This approach is very efficient when 8 or 16 bit pixels are used because the histogram can be represented as an array and the histogram updated by incrementing or decrementing the appropriate bins. Using place holders to track the current maximum or minimum increases performance. More sophisticated histogram representations are necessary for larger pixel types. Our implementation uses c++ maps, which is an extension to the original paper.

This methodology reduces the complexity from $O(n^d)$ to $O(n^{d-1})$, while keeping the structuring element identical to the direct implementation.

3.2 Decomposition of structuring elements

Morphological erosions and dilations are separable – successive dilation by orthogonal lines is equivalent to dilation by a rectangle with sides equal to the line lengths. This means that any hyper-rectangular structuring element can be constructed using several orthogonal lines, typically parallel to the axes.

Approximations of more complex shapes, notably circles and ellipses can be constructed using a number of lines at evenly spaced angles [2]. It is difficult to create a structuring element with a precisely defined radius using this method because line structuring elements from which the circle structuring element is composed must have odd length and there are practical limits due to the realities of underlying digital grid representation of images. In addition it is possible that the structuring elements may not be truly translation invariant due to the representation of line (e.g. Bresenham) used in the decomposition. However, precisely defined radii are rarely critical when a large structuring element is called for. An example of a structuring element created using line structuring elements is shown in Figure 1. Composition of regular shapes, such as hexagons and octagons is more accurate.



Figure 1: Approximate circular structuring element, radius 25, constructed using 8 lines.

It is also possible, in theory, to construct 3D structuring elements in similar ways. The construction of a hyper-rectangle is trivial, however construction of spheres is more problematic. The code discussed later provides preliminary implementations based on some platonic solids and various spherical approximations, but further testing and development is needed.

3.3 Line structuring elements

The decompositions discussed above are important because an efficient, recursive, implementation of erosion and dilations along lines exists. This method was introduced in [6, 12] and can compute an erosion or dilation in 3 operations per pixel, independent of structuring element length. [5] recently reduced the cost to 1.5 pixels per pixel, but the procedure is more complicated and there are reports of no speedup in practice.

The original algorithms utilize forward and backward running maxima (for dilation) for the length of the structuring element from a pixel of interest. The dilation can then be computed for a region the size of the structuring element around the point of interest by comparing values on the running extrema that are separated by the structuring element length. This is illustrated in Figure 2

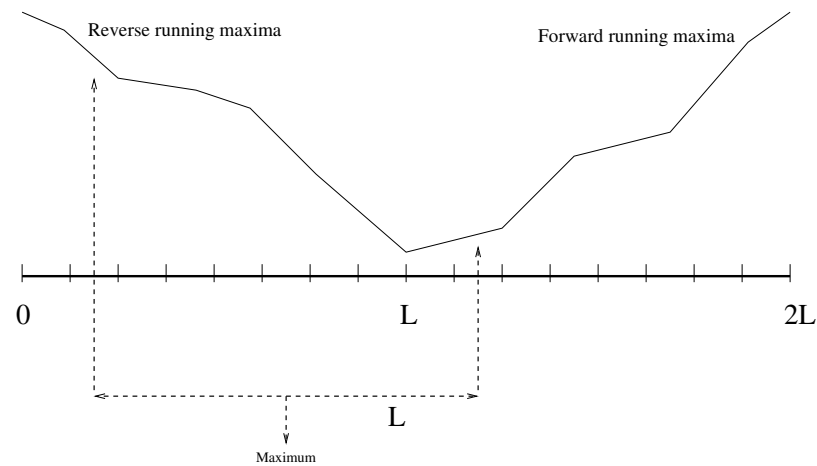


Figure 2: The van Herk, Gil, Werman method.

A method known as *anchor morphology* has been published recently [10] that offers improved performance and the ability to perform a line opening directly (rather than using an erosion/dilation cascade). This method has been implemented in the filters discussed later in the article, but performance issues are not yet clear. The method employs histograms and therefore needs more complex data structures when applied to higher precision data, potentially reducing any speed advantage.

4 Rank filters

Efficient implementations of median and rank filters can be carried out using exactly the same approach as discussed for morphological operations with arbitrary structuring elements. The method was originally proposed in [7]. The implementation discussed later supports arbitrary kernel shapes and pixel types as well as any choice of rank.

Rank filters are not separable. However the performance benefits offered by separability make it worth pretending they are. If median filtering is being used to provide robust noise filtering or background estimation then a separable approximation is worth testing. This concept was originally proposed in [9]. In fact it is also possible to apply the decomposition discussed in Section 3.2 to median filters to achieve a closer approximation to circular kernels.

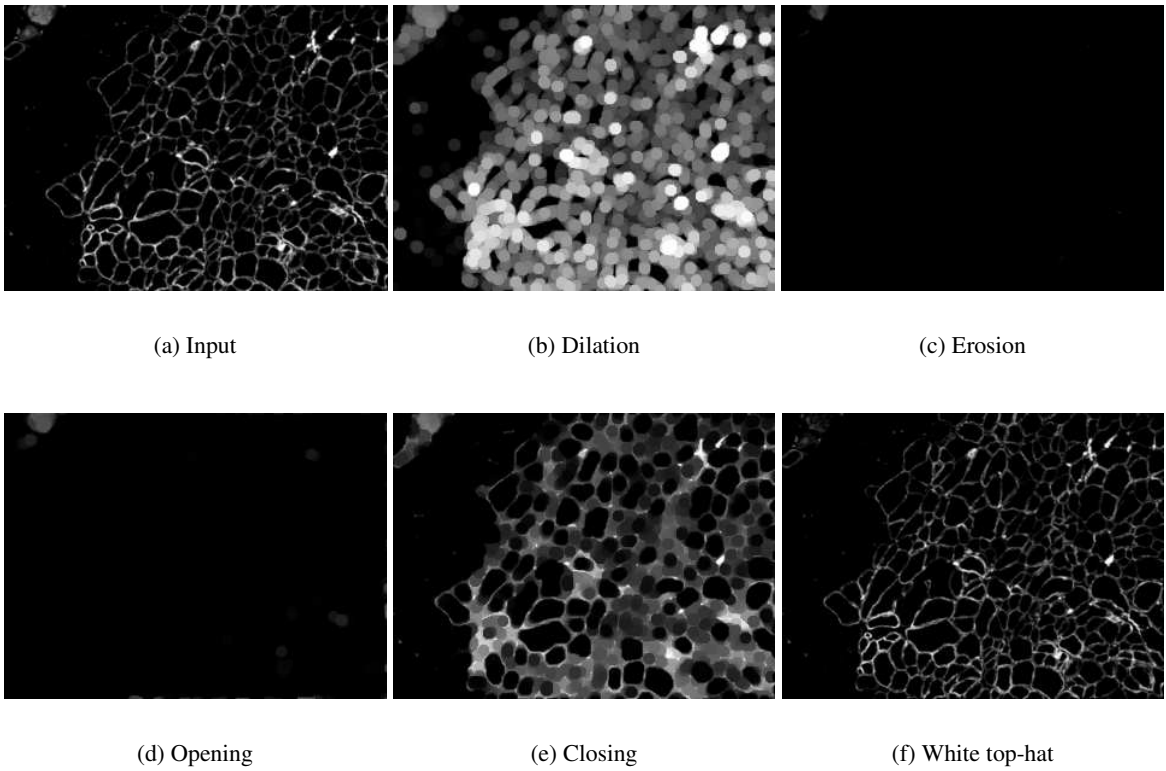


Figure 3: Effect of a dilation (b), an erosion (c), an opening (d), a closing (e) and a white top hat (f) with a ball structuring element.

5 Mean and standard deviation filters

A simplified version of the moving histogram approach can also be used to efficiently compute the mean or standard deviation of an arbitrarily shaped kernel. The histogram used for morphology and rank filters is a data structure that, once established for one pixel, can be easily updated to represent the kernel for a neighboring pixel. The data structure required to perform the equivalent function for mean and variance operations is much simpler – all that is necessary is the sum of pixel values under the kernel (or sum of squared values for variance calculations), and the kernel size. The sum can be updated by adding the new values and subtracting the old and the output computed by dividing by the kernel size.

A more efficient strategy was proposed in [3] for rectangular kernels. This approach first computes an accumulator image in which each i, j is replaced by the sum of voxels “left” and “above” it. This accumulator image may be computed recursively using local neighborhood values. The mean of rectangles of any size may then be computed using accumulated values at the rectangle corners. Figures 4 and 5 illustrate the 2D case and the update formulas are provided in Equations 1, 2, and 3.

$$\begin{aligned} b_{i,j} &= \sum_{x \leq i, y \leq j} a_{x,y} \\ &= b_{i,j-1} + b_{i-1,j} + a_{i,j} - b_{i-1,j-1} \end{aligned} \quad (1)$$

where $b_{i,j}$ is the accumulator value at location i, j and $a_{i,j}$ is the input image intensity at i, j .

$$S_{i,j} = b_{i+w/2, j+h/2} + b_{i-w/2, j-h/2} - b_{i-w/2, j+h/2} + b_{i+w/2, j-h/2} \quad (2)$$

where $S_{i,j}$ is the sum of the pixel values in the neighborhood centered at i, j .

$$m_{i,j} = \frac{1}{w \cdot h} S_{i,j} \quad (3)$$

where $m_{i,j}$ is the output of the mean filter at location i, j .

Using the same strategy, the standard deviation can be efficiently computed. It requires an accumulator image of the squared pixels values, which can be efficiently computed at the same time as the original accumulator image. The update formulas are provided in Equations 4, 5 and 6.

$$\begin{aligned} b2_{i,j} &= \sum_{x \leq i, y \leq j} a_{x,y}^2 \\ &= b2_{i,j-1} + b2_{i-1,j} + a_{i,j}^2 - b2_{i-1,j-1} \end{aligned} \quad (4)$$

where $b2_{i,j}$ is the accumulator value at location i, j for the square image, and $a_{i,j}$ is the input image intensity at i, j .

$$S2_{i,j} = b2_{i+w/2, j+h/2} + b2_{i-w/2, j-h/2} - b2_{i-w/2, j+h/2} + b2_{i+w/2, j-h/2} \quad (5)$$

where $S2_{i,j}$ is the sum of the squared pixel values in the neighborhood centered at i, j .

$$\sigma_{i,j} = \sqrt{\frac{S2_{i,j} - \frac{S_{i,j}^2}{w \cdot h}}{w \cdot h - 1}} \quad (6)$$

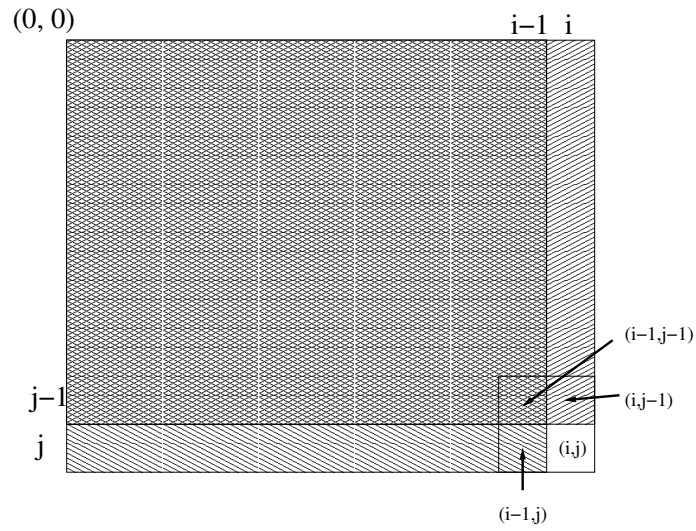


Figure 4: Recursive computation of the accumulator image - value at (i, j) computed using Equation 1. The double hashed region is subtracted because it is included in both $b_{i,j-1}$ and $b_{i-1,j}$.

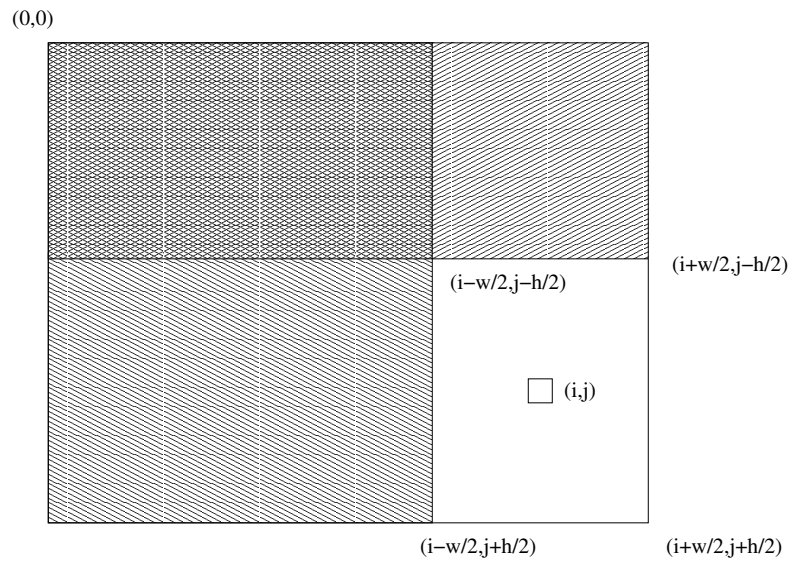


Figure 5: Computation of mean using the accumulated image - value at (i, j) computed using Equation 3.

where $\sigma_{i,j}$ is the output of the standard deviation filter at location i, j .

This approach to convolution has been used recently in face detection applications [13], where rectangular filters of many different sizes and shapes were needed and could be computed from the same accumulation image.

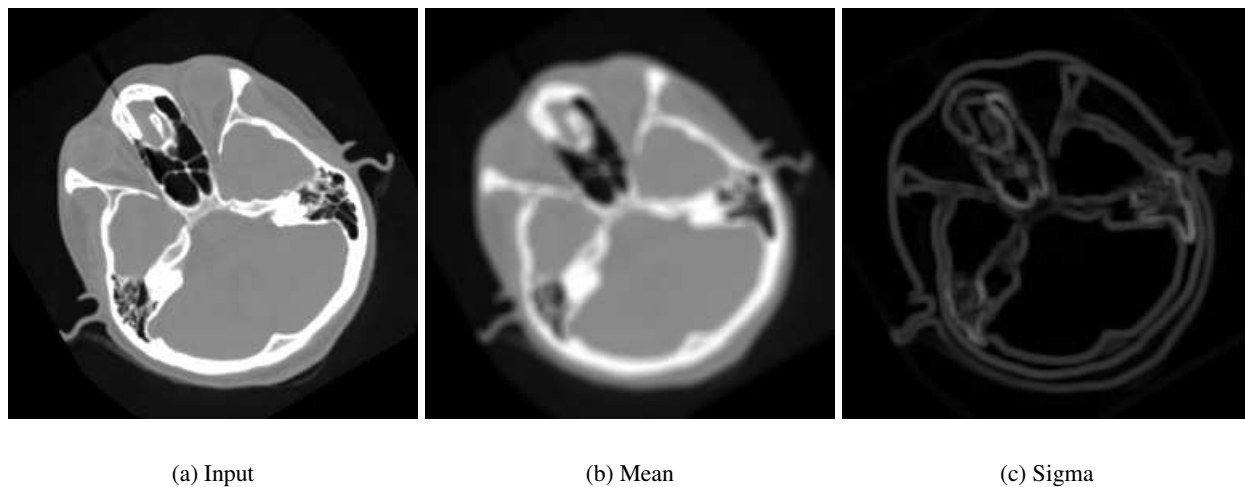


Figure 6: A mean transform (b) and a standard deviation transform (c) with a kernel of radius 3.

6 ITK implementation

The filters discussed in this article are contained in 3 packages – *consolidatedMorphology*¹, *fastRankMean* and *boxConvolution*. The most recent versions of these packages can be obtained from <http://voxel.jouy.inra.fr/darcsweb/>². All of the packages include multithreaded filters and include many examples and tests. Unless indicated otherwise, all filters will behave basically the same way as other kernel filters, requiring either a radius or a neighborhood to be specified.

6.1 Common filters

All the filters provided with those packages are implemented as subclasses of one of two new classes: *itk::BoxImageFilter* and *itk::KernelImageFilter*. *itk::BoxImageFilter* is a subclass of *itk::ImageToImageFilter* and provides some features used in all the box based filters:

- the management of the radius of the box,
- and the enlargement of the input requested region, according to the box size.

¹An earlier version of the *consolidatedMorphology* package has been submitted to the InsightJournal. However many improvements and bug fixes have been included since then.

²The most recent versions can be obtained using darcs [1] with the command *darcs get http://voxel.jouy.inra.fr/darcs/contrib-itk/package*, where *package* must be replaced by *consolidatedMorphology*, *fastRankMean* or *boxConvolution*.

itk::KernelImageFilter is a subclass of *itk::BoxImageFilter*, and provides some features used in all the kernel based filters, in addition to the features of the *itk::BoxImageFilter* class:

- the management of the kernel,
- a redefined `SetRadius()` method to create a box kernel with the provided radius,
- a default box kernel of radius 1³.

A third filter, *itk::SeparableImageFilter*, is used to easily implement a separable version of an algorithm, by using its basic implementation in a subclass of *itk::BoxImageFilter*, or any other subclass of *ImageToImageFilter* with a `SetRadius()` method.

Some filters already in ITK have been modified to use *itk::BoxImageFilter* or *itk::KernelImageFilter*⁴. Their API is not modified.

6.2 Morphology filters – consolidatedMorphology

The morphology filters utilize a new class – *FlatStructuringElement* to describe, arbitrary and decomposable structuring elements. It provides the following methods to create structuring elements with different characteristics:

- `Ball()` generate a ball structuring element (a circle in 2D). It takes the radius of the structuring element as parameter.
- `Box()` produces a box structuring element. It takes the radius of the structuring element as parameter.
- `Poly()` produces an approximation to a circle or sphere using line structuring elements, taking the desired radius and number of lines as parameters. In the 3D case an approximation of a sphere will be attempted. Caution is advised because this is not well tested yet.
- `Cross()` produces a cross structuring element. It takes the radius of the structuring element as parameter.
- `Annulus()` produces an annulus structuring element. It takes the radius of the structuring element as parameter, as well as the thickness of the annulus, and a boolean to indicate whether the center neighbors should be set inside the neighborhood or not⁵.
- `FromImage()` produces a structuring element from an image. The image is passed as parameter to the method. A optional parameter can also be passed: the pixel value to be considered as the foreground value in the image. This value defaults to `NumericTraits< PixelType >::max()`. This lets the user visualize the structuring element.

The algorithm used by a filter is set by the `SetAlgorithm` method, with options of *BASIC*, *HISTO*, *VHGW* and *ANCHOR*, for the traditional ITK implementation, the moving histogram algorithm, the van Herk, Gil, Werman algorithm and the anchor algorithm respectively. The VHGW and ANCHOR algorithms can only

³This feature should help many ITK beginners who are often *not* providing a structuring element to the morphology filters, and thus get difficultly understandable crashes.

⁴`itk::MedianImageFilter`, `itkMeanImageFilter`, `itk::NoiseImageFilter` and `itk::MorphologyImageFilter`.

⁵The *Annulus()* constructor is a contribution of Dan Mueller.

be used for Box and Poly structuring elements. VHGW is more thoroughly tested. The HISTO algorithm produces the identical results to BASIC, and is always faster. It is the default and should be used if you need precisely defined, non rectangular, structuring elements. If a Box structuring element is needed then VHGW or ANCHOR should be used, as they offer the best performance and are exact in that case. Poly structuring elements are approximations of circles that will offer improved performance with VHGW or ANCHOR algorithms, but the user will need to consider whether the approximation is suitable for the application in question.

The availability of line morphology operations means that new operations, such as “union of openings” can be implemented easily.

6.3 Rank and mean filters – fastRankMean

The *fastRankMean* package uses the sliding window method to implement rank and mean filters for arbitrary kernel shapes. It also uses line versions of these kernels to provide a “separable rank” filter – an fast approximation to a real rank filter as discussed in Section 4. There are also a number of filters that accept a mask input and return the rank or mean value of the intersection of kernel and mask. These are experimental and haven’t been thoroughly tested. The filters are *itkRankImageFilter*, *itkMovingWindowMeanImageFilter*, *itkFastApproxRankImageFilter*, *itkFastApproxMaskRankImageFilter* and *itkMaskedRankImageFilter*. *itkRankImageFilter* implements arbitrary shaped kernels, *itkFastApproxRankImageFilter* implements the separable approximation and *itkMovingWindowMeanImageFilter* implements an arbitrary shaped kernel mean.

6.4 Rectangular convolution – boxConvolution

The *boxConvolution* uses the accumulation method described in Section 5 to implement rectangular mean and variance computations. The filters implement different boundary conditions to *itkMeanImageFilter*, with the mean of the kernel inside the image being computed. The filters in this package are multithreaded and deal with arbitrary dimensions. The current filters do not support the mode of operation used in face recognition application in which an accumulation image is repeatedly “queried” for mean values of various sized kernels. However introducing such a capability is relatively easy.

6.5 Extended languages support

All the new filters provided are wrapped using WrapITK’s external projects [4] and have been successfully tested with python.

7 Performance

All the execution times in this section are measured on a computer with four Intel®Xeon®CPU cores at 2.33GHz with 4MB cache, running CentOS 4.4 64 bits. Unless specified in the description, the tests are forced to run on a single core.

7.1 Morphology

Execution times for the dilation, the opening, and the gradient transform are shown in Tables 1, 3 and 2, and in Figure 7. The predicted linear complexity for the number of neighbors is observed for the basic algorithm, as well as the constant complexity of the van Herk / Gil Werman and the anchor algorithm. The linear complexity for the number of pixels added and removed per translation is observed for the moving histogram algorithm, as expected.

A good threading support is observed for all the implementations, as shown in Table 4 and Figure 7.

7.2 Rank and Mean filters

Relative times for sliding window median and mean filters and separable median filters are shown in Tables 6 and 7 and in Figure 8. The predicted linear complexity is observed for the sliding window approaches (complexity of direct approach is $O(n^2)$ in 2D, reduced to $O(n)$ by using the sliding window. The separable median exhibits a runtime independent of kernel size, as expected.

7.3 Box Convolution

The relative times for optimized and standard convolution are shown in Table 9 and Figure 9, and demonstrate significantly improved performance for kernel radii greater than 1. The times support the theoretical prediction that the complexity of the algorithm is independent of kernel size.

A good threading support is observed for all the implementations, as shown in Table 10 and Figure 9.

7.4 Timing notes

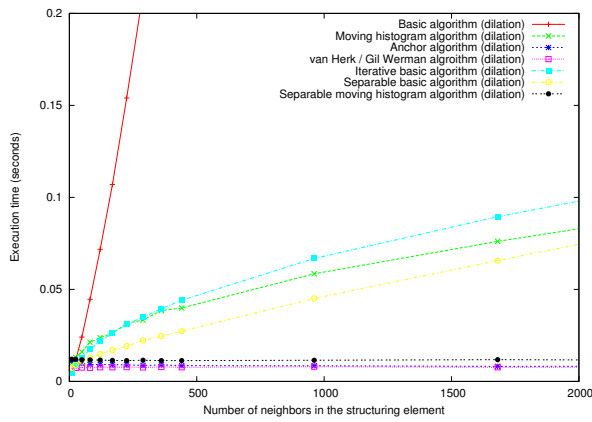
You may have noticed that the optimized filters of radius 1 seem to regularly perform slower than their larger counterparts. We can think of no reason for this. The algorithms that have kernel size independent complexity should not be slower for small kernels than large ones because the only difference occurs at borders and when the sliding window is being created, and both situations favour small kernels. We can only guess that there are caching issues involved.

8 Implementation Notes

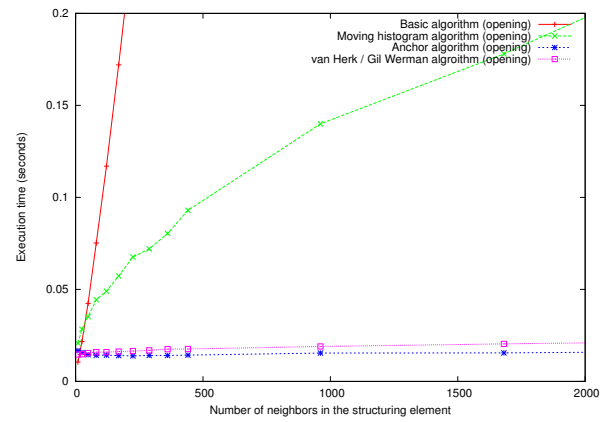
A lot of effort has been spent implementing and optimizing these filters while attempting to maintain good ITK style. This section summarizes some observations and experiences:

8.1 Moving histograms

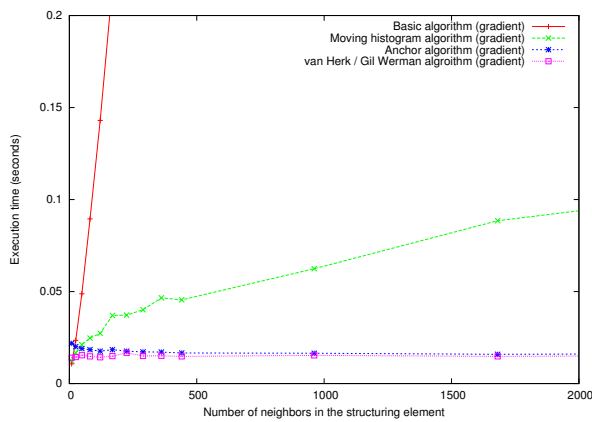
The most obvious way of implementing moving histograms involves neighborhood iterators. However the resulting performance wasn't good – it appears that neighborhood iterator complexity is proportional to radius rather than the number of active neighbors. A method using lists of offsets combined with image Get/SetPixel methods approach was used instead.



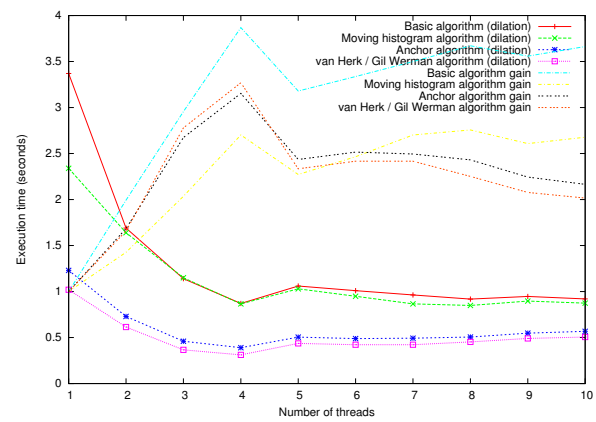
(a) Dilation



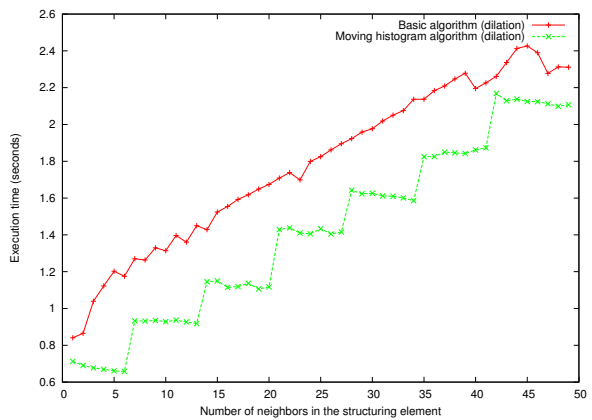
(b) Opening



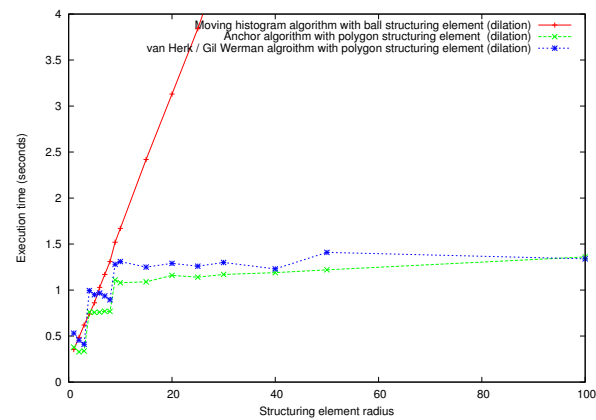
(c) Gradient



(d) Threads

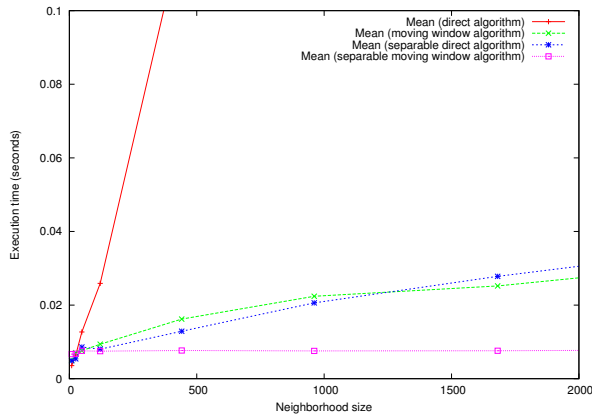


(e) Number of neighbors

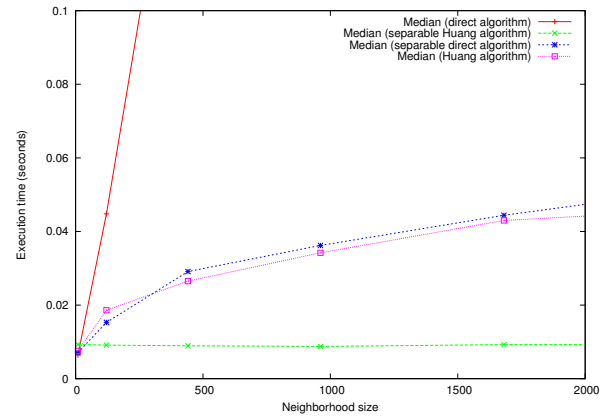


(f) Polygon

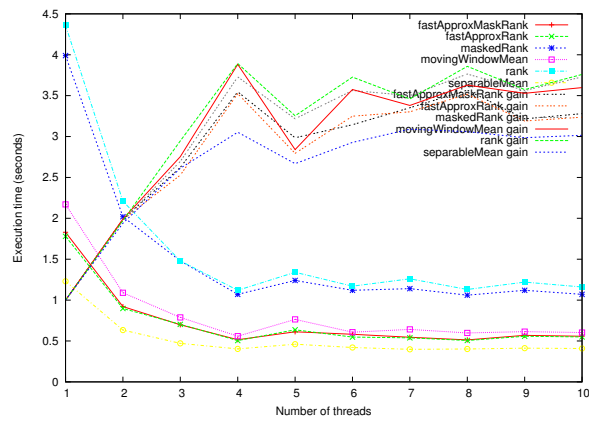
Figure 7: Execution times with a box structuring element of increasing size for different algorithms of dilation (a), opening (b) and gradient (c). Execution times with and increasing number fo threads (d). Execution times with an increasing number of neighbors in a box structuring of constant radius (e). Execution times with a polygon structuring element. The polygon approximations use the default number of lines (a maximum of 6 when radius is greater than 8 (f)). Results are reported in Tables 1, 3, 2, 4 and 5.



(a) Mean



(b) Median



(c) Threads

Figure 8: Execution times for an increasing kernel size with several algorithms of mean filters (a) and median filters (b). Execution times with an an increasing number of threads (c). Results are reported in Tables 6, 7 and 8.

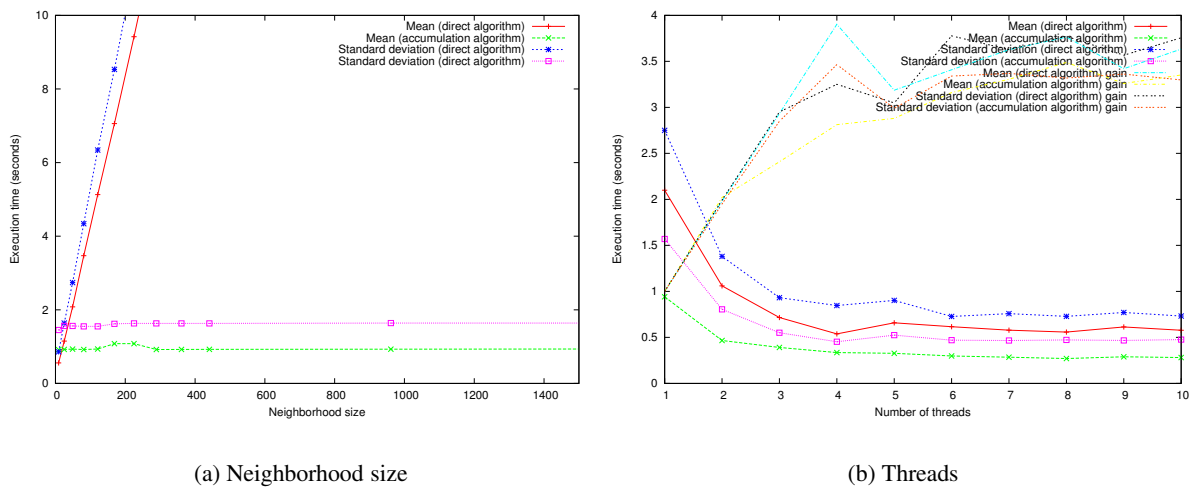


Figure 9: Execution times for and increasing kernel size (a), and an increasing number of threads (b). Results are reported in Tables 9 and 10

The original paper recommended moving the window in a zig-zag pattern, i.e horizontally across a the first row, down a step to the second row and then back, but this involves accessing data in a reverse raster order which can potentially reduce cache performance. An alternative has been implemented that always moves the window in forward raster direction, at the cost of additional histogram copies, has been implemented and exhibits improved performance for large images. Differences for small images weren't detectable.

8.2 16 bit data types

Histograms for 16 bit data types can be implemented using arrays or maps. One would expect arrays to offer a simpler and therefore faster implementation, but our results have been mixed. Presumably the performance depends significantly on voxel statistics.

8.3 Line Operations

The van Herk/Gil and Werman and anchor methods operate on image transects, potentially at any angle. The transect data needs to be extracted from the image and the processed transect written back, with successive parallel transects being processed. Existing iterators don't do this particularly efficiently, so image Get/Set-Pixel operations are being used. This approach isn't ideal either and needs to be worked on. In general there is no need for boundary checks because the intersection between transect and image region is calculated, so a potentially random access method without boundary checks would be ideal.

Building dimension independent code also adds complexity to this filter which can be avoided in dimension specific implementations. The process of sweeping the transect across the image region is much more complex (and therefore slower) when written in a dimension independent fashion.

The standard ITK threading approach isn't ideal for this style of filtering either – a better option would be splitting the image based on transects instead of blocks. Obviously this sort of change isn't practical.

8.4 Refactoring

The three packages do share some components, and some refactoring is called for. This most widely used components are histograms and sliding window infrastructure, which need to be consolidated.

9 Comments and Conclusions

This article has provided background theory for and implementations of a number of important approaches to kernel based filtering. These methods significantly reduce complexity and execution time, by some orders of magnitude in many cases. These approaches are all well established in the literature but weren't available in ITK. Availability of filtering algorithms which are always fast, irrespective of the kernel size, can make much simpler approaches to many problems practical.

10 Acknowledgments

We thank Dr Pierre Adenot and MIMA2 confocal facilities (<http://mima2.jouy.inra.fr>) for providing the 3D test image. We are grateful to the INRA MIGALE bioinformatics platform (<http://migale.jouy.inra.fr>) for providing the computational resources used for the timing tests.

References

- [1] <http://www.darcs.net>. 2
- [2] R. Adams. Radial decomposition of discs and spheres. *CVGIP: Graphical models and image processing*, 55(5):325–332, September 1993. 3.2
- [3] F.C. Crow. Summed-area tables for texture mapping. In *SIGGRAPH '84: Proceedings of the 11th annual conference on Computer graphics and interactive techniques*, pages 207–212, New York, NY, USA, 1984. ACM Press. 5
- [4] Zachary Pincus Gaëtan Lehmann and Benoit Regrain. Wrapitk - enhanced languages support for the insight toolkit. *Insight Journal*, January - June 2006. 6.5
- [5] J. Gil and R. Kimmel. Efficient dilation, erosion, opening and closing algorithms. In *Mathematical Morphology and its Applications to Image and Signal Processing*, pages 301–310. Kluwer Acad. Pub, 2000. 3.3
- [6] J. Gil and M. Werman. Computing 2-d min, median, and max filters. *IEEE Transactions on Pattern Analysis and Machine Intelligence*, 15(5):504–507, May 1993. 3.3
- [7] T.S. Huang, G.Y. Yang, and G.Y. Tang. A fast two-dimensional median filtering algorithm. *IEEE Transactions on Acoustics, Speech and Signal Processing*, 27:13–18, 1979. 4
- [8] L. Ibanez and W. Schroeder. *The ITK Software Guide*. Kitware, Inc. ISBN 1-930934-10-6, <http://www.itk.org/ItkSoftwareGuide.pdf>, 2003.

- [9] P.M. Narendra. A separable median filter for image noise smoothing. *IEEE Transactions on Pattern Analysis and Machine Intelligence*, 3:20–29, 1981. [4](#)
- [10] M. Van Droogenbroeck and M. Buckley. Morphological erosions and openings: fast algorithms based on anchors. *Journal of Mathematical Imaging and Vision, Special Issue on Mathematical Morphology after 40 Years*, 22(2-3):121–142, May 2005. Algorithms in ANSI C code are available in libmorpho. [3.3](#)
- [11] M. Van Droogenbroeck and H. Talbot. Fast computation of morphological operations with arbitrary structuring elements. *Pattern Recognition Letters*, 17(14):1451–1460, 1996. [3.1](#)
- [12] M. van Herk. A fast algorithm for local minimum and maximum filters on rectangular and octagonal kernels. *Pattern Recognition Letters*, 13(7):517–521, July 1992. [3.3](#)
- [13] P. Viola and M. Jones. Robust real-time face detection. *International Journal of Computer Vision*, 57(2):137–154, 2004. [5](#)

Appendix

Radius	Basic	Iterative	Separable	Histogram	Separable histogram	Anchor	van Herk / Gil Werman
1	0.00437	0.00436	0.00734	0.00987	0.0121	0.0111	0.00715
2	0.0118	0.00872	0.00901	0.0131	0.0121	0.0101	0.00733
3	0.0241	0.013	0.0108	0.0161	0.0118	0.00979	0.00756
4	0.0446	0.0175	0.0127	0.0213	0.0117	0.00922	0.00736
5	0.0718	0.0219	0.0149	0.0237	0.0116	0.00923	0.00768
6	0.107	0.0262	0.017	0.0262	0.0114	0.00906	0.00768
7	0.154	0.0311	0.0192	0.0315	0.0113	0.00899	0.00779
8	0.211	0.0349	0.0223	0.0334	0.0115	0.00865	0.00759
9	0.281	0.0395	0.0246	0.0385	0.0113	0.00892	0.00784
10	0.365	0.0441	0.0273	0.0399	0.0113	0.0086	0.00767
15	1.03	0.0668	0.0451	0.0585	0.0115	0.00851	0.00798
20	2.23	0.0895	0.0657	0.0761	0.0118	0.00819	0.0077
25	4.11	0.114	0.0911	0.0958	0.0114	0.00826	0.00778
30	6.84	0.139	0.121	0.108	0.0115	0.00847	0.00801
40	15.5	0.194	0.195	0.145	0.0116	0.00872	0.00811
50	29.4	0.257	0.283	0.185	0.0118	0.00858	0.00798
100	227	0.719	0.974	0.348	0.0127	0.00858	0.0082

Table 1: Execution times in seconds for dilation by boxes using several algorithm implementations applied to the 256×256 cthead image.

Radius	Basic	Histogram	Anchor	van Herk / Gil Werman
1	0.0107	0.0124	0.0219	0.014
2	0.0235	0.0167	0.0201	0.0144
3	0.0488	0.0211	0.019	0.0154
4	0.0895	0.0247	0.0184	0.0148
5	0.143	0.0273	0.0176	0.0143
6	0.216	0.037	0.0184	0.0149
7	0.308	0.0372	0.0176	0.0167
8	0.423	0.0401	0.0172	0.015
9	0.563	0.0466	0.0171	0.0151
10	0.73	0.0455	0.0166	0.0148
15	2.07	0.0624	0.0165	0.0153
20	4.46	0.0885	0.0159	0.0148
25	8.22	0.104	0.0163	0.0153
30	13.6	0.118	0.0161	0.0151
40	30.9	0.153	0.0163	0.0153
50	58.6	0.196	0.0168	0.0156
100	452	0.339	0.0163	0.0157

Table 2: Execution times in seconds for morphological gradient transformation by boxes using several algorithm implementations applied to the 256×256 cthead image.

Radius	Basic	Histogram	Anchor	van Herk / Gil Werman
1	0.0105	0.0208	0.0167	0.0146
2	0.0217	0.0283	0.0157	0.0148
3	0.0424	0.0352	0.0145	0.0154
4	0.0752	0.0444	0.0142	0.0159
5	0.117	0.049	0.0143	0.0159
6	0.172	0.0573	0.014	0.0162
7	0.24	0.0676	0.0139	0.0165
8	0.324	0.072	0.0141	0.0169
9	0.425	0.0804	0.0141	0.0175
10	0.546	0.093	0.0143	0.0176
15	1.5	0.14	0.0154	0.019
20	3.19	0.178	0.0155	0.0204
25	5.9	0.235	0.0164	0.0219
30	9.9	0.274	0.0175	0.0236
40	23	0.383	0.0193	0.0272
50	45.3	0.522	0.0213	0.0298
100	421	1.6	0.0346	0.0493

Table 3: Execution times in seconds for morphological opening by boxes using several algorithm implementations applied to the 256×256 cthead image.

Threads	Basic	Histogram	Anchor	van Herk / Gil Werman
1	3.37	2.34	1.23	1.02
2	1.69	1.64	0.73	0.615
3	1.14	1.15	0.46	0.367
4	0.871	0.866	0.39	0.312
5	1.06	1.03	0.505	0.437
6	1.01	0.949	0.489	0.422
7	0.963	0.866	0.493	0.422
8	0.918	0.849	0.506	0.453
9	0.947	0.897	0.548	0.491
10	0.92	0.874	0.568	0.506

Table 4: Execution times in seconds for morphological opening by boxes using several algorithm implementations applied to the 3200×2400 image.

Radius	Histogram	van Herk / Gil Werman	Anchorn
1	0.354	0.379	0.532
2	0.486	0.329	0.455
3	0.62	0.338	0.411
4	0.74	0.763	0.995
5	0.862	0.757	0.95
6	1.03	0.759	0.968
7	1.17	0.77	0.936
8	1.31	0.768	0.894
9	1.52	1.11	1.28
10	1.67	1.08	1.31
15	2.42	1.09	1.25
20	3.13	1.16	1.29
25	3.84	1.14	1.26
30	4.64	1.17	1.3
40	5.95	1.19	1.23
50	7.6	1.22	1.41
100	19	1.36	1.34

Table 5: Execution times in seconds for morphological opening by boxes using several algorithm implementations applied to the 256×256 cthead image.

Radius	Direct	Moving window	Separable direct	Separable moving window
1	0.00355	0.00498	0.00487	0.00668
2	0.00642	0.00706	0.0054	0.00679
3	0.0127	0.00761	0.00861	0.00756
5	0.0259	0.00936	0.00803	0.00749
10	0.121	0.0162	0.0129	0.00765
15	0.35	0.0224	0.0206	0.00755
20	0.771	0.0252	0.0278	0.0076
40	5.59	0.059	0.0699	0.00871

Table 6: Execution times in seconds for mean filters using direct and sliding window implementations applied to the 256×256 cthead image.

Radius	Direct	Huang	Separable direct	Separable huang
1	0.00642	0.00758	0.0071	0.0093
5	0.0448	0.0186	0.0153	0.00913
10	0.177	0.0265	0.0291	0.00895
15	0.445	0.0342	0.0362	0.00876
20	0.93	0.043	0.0444	0.00925
40	6.21	0.061	0.0899	0.00936

Table 7: Execution times in seconds for median filters using direct and sliding window implementations applied to the 256×256 cthead image. The separable median is an approximation and therefore doesn't produce the same result as the direct or sliding algorithms.

Threads	fastApproxMaskRank	fastApproxRank	maskedRank	movingWindowMean	rank	separableMean
1	1.83	1.78	3.99	2.17	4.36	1.23
2	0.921	0.898	2.02	1.09	2.21	0.634
3	0.698	0.704	1.48	0.788	1.48	0.471
4	0.516	0.505	1.07	0.559	1.12	0.403
5	0.613	0.637	1.24	0.764	1.34	0.461
6	0.582	0.548	1.12	0.607	1.17	0.42
7	0.546	0.539	1.14	0.642	1.26	0.398
8	0.513	0.506	1.06	0.598	1.13	0.402
9	0.569	0.558	1.12	0.615	1.22	0.412
10	0.558	0.55	1.07	0.603	1.16	0.408

Table 8: Execution times in seconds for median and mean filters using direct and sliding window implementations applied to the 3200×2400 image.

Size	Direct Mean	Box Mean	Direct sigma	Box sigma
1	0.557	0.916	0.858	1.45
2	1.15	0.924	1.64	1.56
3	2.08	0.932	2.74	1.56
4	3.47	0.92	4.34	1.55
5	5.13	0.935	6.34	1.55
6	7.06	1.08	8.53	1.62
7	9.42	1.08	11.3	1.63
8	12.2	0.922	14.5	1.63
9	15.3	0.924	18	1.63
10	18.9	0.925	22.1	1.63
15	43.3	0.929	50.2	1.64
20	80.1	0.936	91.8	1.64
25	131	0.939	149	1.64

Table 9: Execution times in seconds for mean and standard deviation using direct and box convolution implementations applied to the 3200×2400 image.

Size	Direct Mean	Box Mean	Direct sigma	Box sigma
1	2.1	0.942	2.75	1.57
2	1.06	0.466	1.38	0.805
3	0.716	0.391	0.932	0.551
4	0.538	0.335	0.846	0.453
5	0.659	0.327	0.902	0.525
6	0.616	0.298	0.728	0.47
7	0.579	0.285	0.758	0.466
8	0.558	0.27	0.729	0.473
9	0.614	0.289	0.771	0.467
10	0.578	0.281	0.732	0.476

Table 10: Execution times in seconds for mean and standard deviation using direct and box convolution implementations applied to the 3200×2400 image.

Efficient implementation of kernel filtering

Richard Beare¹ and Gaëtan Lehmann²

¹Department of Medicine, Monash University, Australia.

²INRA, UMR 1198; ENVA; CNRS, FRE 2857, Biologie du Développement et
Reproduction, Jouy en Josas, F-78350, France

Introduction

- Describe methods that reduce computational complexity of kernel filters by orders of magnitude.
- Discuss the tradeoffs that need to be considered when using these methods.

Motivation

Large median filter 111×111 for background estimation in microscopy image.

- Direct implementation takes at least 20 minutes.
- Efficient approximation takes less than 5 seconds.

Improving filter performance

- Recursive computation

Improving filter performance

- Recursive computation
 - An output value can be computed based on a neighbouring output.

Improving filter performance

- Recursive computation
 - An output value can be computed based on a neighbouring output.
 - This reduces complexity by eliminating repeated computation.

Improving filter performance

- Recursive computation
 - An output value can be computed based on a neighbouring output.
 - This reduces complexity by eliminating repeated computation.
- Separability

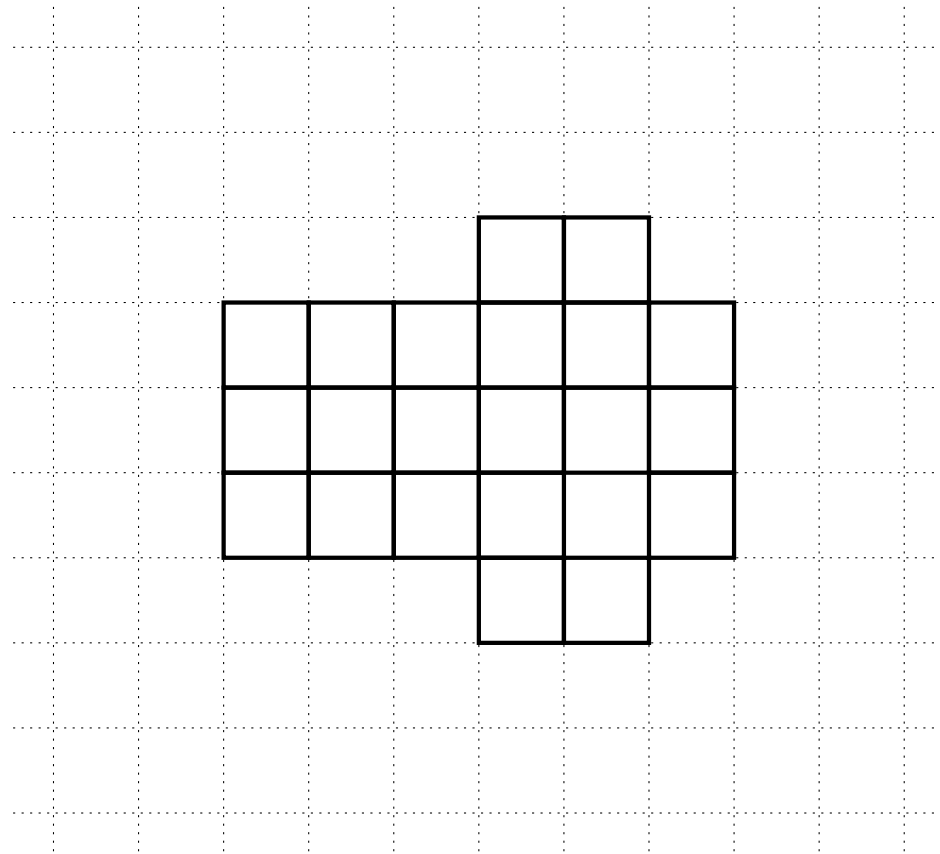
Improving filter performance

- Recursive computation
 - An output value can be computed based on a neighbouring output.
 - This reduces complexity by eliminating repeated computation.
- Separability
 - Certain multidimensional kernels can be decomposed into a number of one dimensional operations.

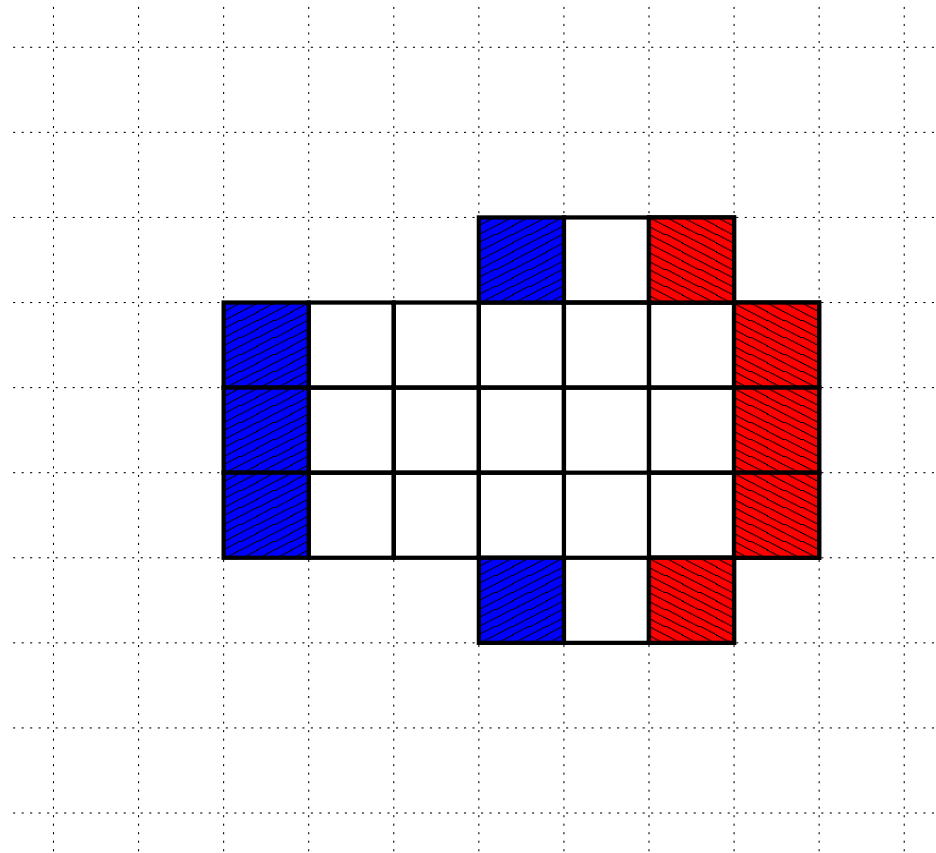
Improving filter performance

- ITK Gaussian filtering classes use both approaches.

Sliding window



Sliding window



Sliding window

- Collect a summary of all pixels in the neighbourhood.
- Compute the output value from the summary.
- Move the window and update the summary.

Sliding window

Reduces complexity from $O(n^d)$ to $O(n^{d-1})$

The standard updatable summaries are:

- Sum or sum of squares for mean and variance computations.
- Histograms for rank filters including mathematical morphology.

Separability/Decomposition

- Some useful filters can be computed using a cascade of operations along lines.

Separability/Decomposition

- Some useful filters can be computed using a cascade of operations along lines.
- Special forms of updateable computations exist for some operations along lines.

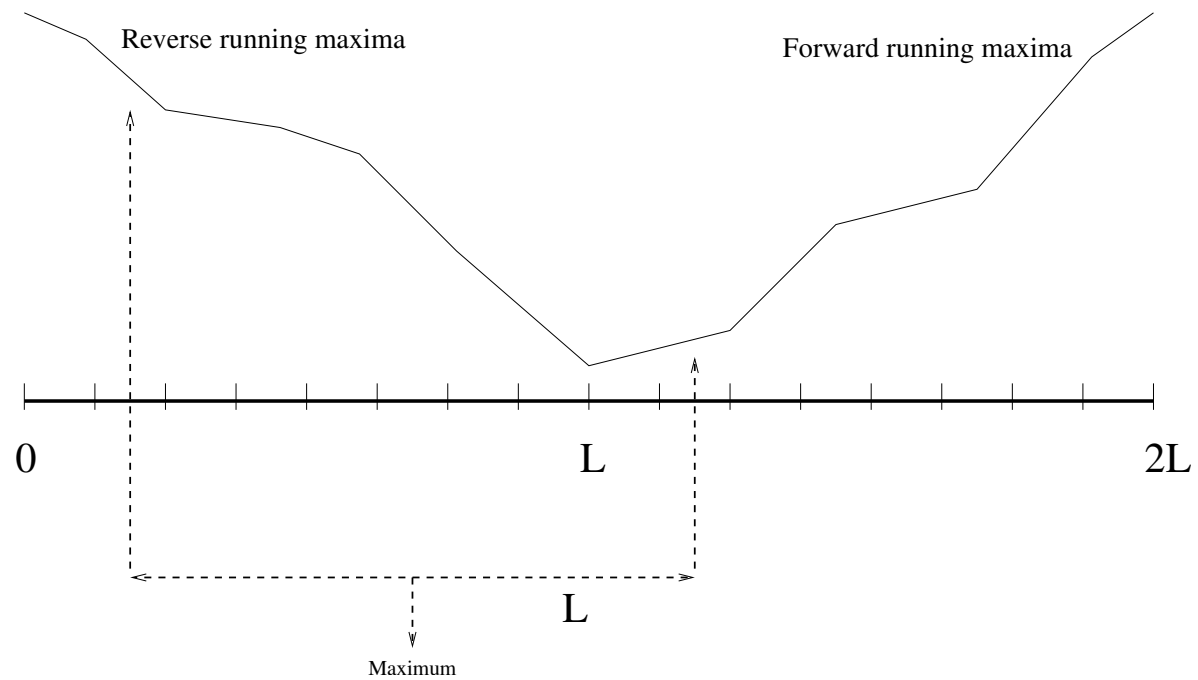
Separability/Decomposition

- Some useful filters can be computed using a cascade of operations along lines.
- Special forms of updateable computations exist for some operations along lines.
- These lead to operations with complexity independent of line length.

Mathematical Morphology

- van Herk/Gil Werman algorithm.
- Erosions/dilations along lines with 3 operations per pixel.

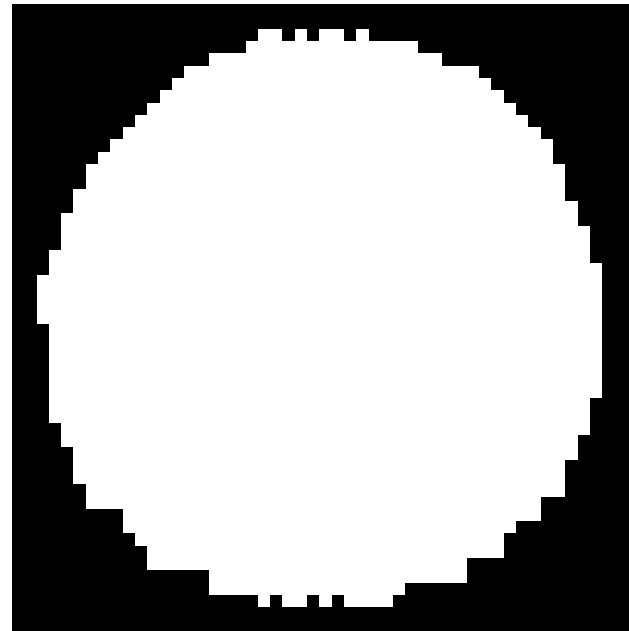
Mathematical Morphology



Mathematical Morphology

- Decomposition of shapes as follows:
 - Hyper-boxes - cascade of line operations parallel to image axes.
 - Approximate circles in 2D.
 - Experimental approximation to spheres.

Mathematical Morphology



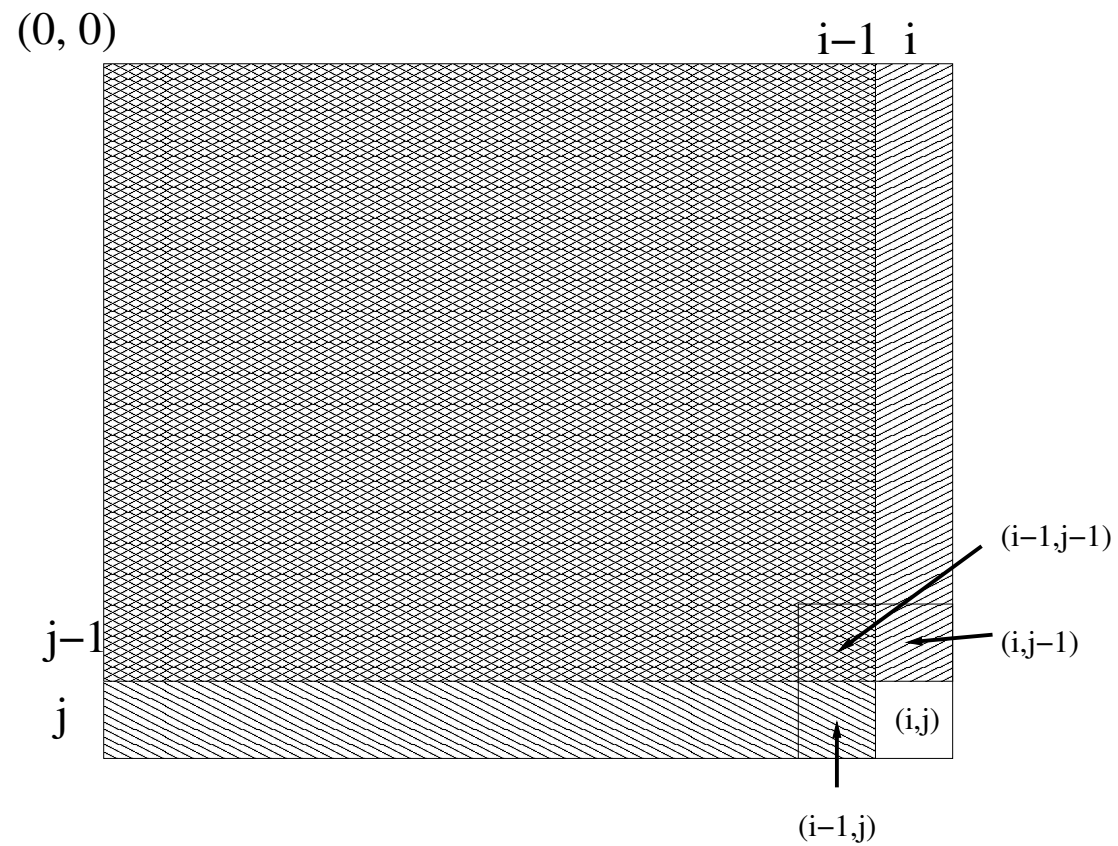
Robust smoothing filters

- Median filters aren't separable.
- Applying a cascade of line based rank filters produces a fast, robust smoother.

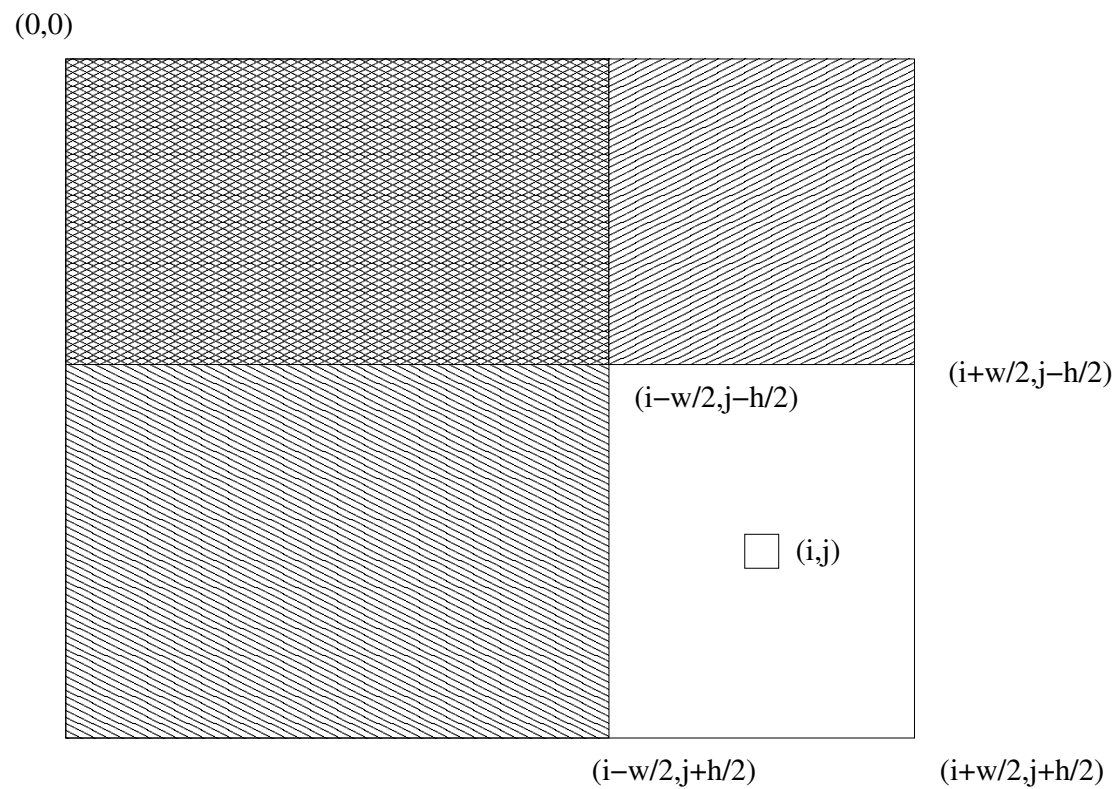
Accumulation image methods

- Useful for sums, means or variances of boxes.
- One accumulation image can be used to evaluate lots of different kernel sizes.
- Can also be used for binary morphology and binary median filters.

Accumulation image methods



Accumulation image methods



Summary of filters

- **Mathematical Morphology using flat structuring elements**
- arbitrary, box, polygon.
- **Accumulation image methods** - mean and standard deviation. Only one kernel size.
- **Rank filters** - arbitrary, boxes - separable approximation, also masked versions.

Summary of complexities

- Sliding window - $O(n^{d-1})$ - arbitrary morphology, arbitrary rank and mean filters.
- Box convolution - constant complexity.
- MM along lines - constant complexity - approximate circles, boxes.
- Rank operations along lines - uses sliding windows and provides a fast, robust smoother.